Title

THE FABRICATION AND SUPERCONDUCTING PROPERTIES OF MULTIFILAMENTARY Nb3Sn WITH A Mg-DOPED BRONZE

Author

Dietderich, D.R.

Publication Date

1983-06-01

Center for Advanced Materials

CAM REPORT

THE FABRICATION AND SUPERCONDUCTING PROPERTIES OF MULTIFILAMENTARY Nb_3Sn WITH A Mg-DOPED BRONZE

D.R. Dietderich
(M.S. Thesis)

June 1983

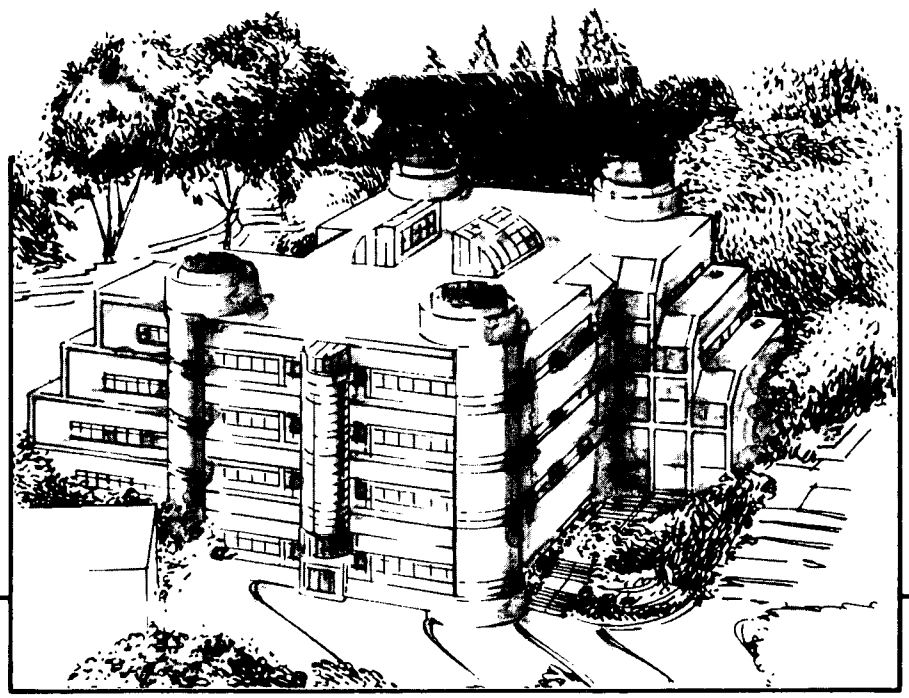

Materials and Chemical Sciences Division

Lawrence Berkeley Laboratory • University of California

ONE CYCLOTRON ROAD, BERKELEY, CA 94720 • (415) 486-4755

Prepared for the U.S. Department of Energy under Contract DE-AC03-76SF00098

DISCLAIMER

THE FABRICATION AND SUPERCONDUCTING PROPERTIES OF MULTIFILAMENTARY Nb_3Sn WITH A Mg-DOPED BRONZE

Daniel Robert Dietderich
M.S. Thesis

Department of Materials Science and Mineral Engineering
University of California, Berkeley

and

Materials and Chemical Sciences Division
Lawrence Berkeley Laboratory
University of California
Berkeley, CA 94720

June 1983

THE FABRICATION AND SUPERCONDUCTING PROPERTIES OF MULTIFILAMENTARY Nb_3Sn WITH A Mg-DOPED BRONZE

Daniel Robert Dietderich
M.S. Thesis

ABSTRACT

Multifilamentary Nb_3Sn superconducting wires were fabricated by the "internal bronze" process. The conductor contained 133 niobium filaments in a Cu-Sn or Cu-Sn-Mg bronze matrix which had a composition of 6.7at.% Sn. Up to 0.62at.% Mg was added to the bronze. The wires were heat treated at aging temperatures between 650-780°C for times up to 20 days. The optimum aging temperature for all wires, that is, for all the compositions, is in the range 700-750°C. The Nb_3Sn formed at different rates in each wire, as a result the optimum aging condition for each wire was different. Near complete filament conversion to Nb_3Sn the Mg-doped wires have much higher normalized critical currents, I_{cNb}, (4.2K,10T) all aging temperatures. However, for some aging temperatures the I_{cNb} of the Mg-free wire is higher than those of the Mg doped wires when compared at partial filament conversion, approximately 50 percent. When the wires with 0.62at.% Mg and no Mg are compared at near complete reaction the Mg doped wire is seen to give a 100-150 percent increase in I_{cNb} for magnetic fields of 10T(4.2K). A 0.10a/o Mg addition to the high tin wire does not increase the critical current density above that of the Mg-free wire for lower aging temperatures, less than 750°C. Since the niobium filaments in the Mg-free wire have a much smaller diameter than those in the Mg-doped wire it appears that filament size, i.e. interface curvature, may play a more dominate role in the Nb_3Sn layer formation. During wire heat treatment essentially all of the magnesium in the bronze diffuses to the Nb_3Sn layer leaving little residual in the matrix. The magnesium distribution across the layer is

not uniform; the magnesium appears to congregate at the Nb_3Sn-bronze interface. The addition of 0.62a/o Mg to the low-tin bronze wire increases the layer growth exponent by a factor of two. This increase most certainly is associated with the change in chemical composition of the Nb_3Sn layer. The new growth mechanism which would produce this increase is not known.

TABLE OF CONTENTS

ACKNOWLEDGEMENTS

I would like to express my deepest gratitude to my advisor, Professor J.W. Morris, Jr., for his close collaboration in this work, and for his guidance, enthusiasm, inspiration, but above all for his patience.

I would also like to express my sincere thanks to Dr. I. W. Wu and J. T. Holthuis for their stimulating discussions, valuable advice, and collaboration in many parts of this work. Their experience made it possible to complete this research. The in-depth discussion with D. Frear and J. Glazer regarding fundamental aspects of the work was appreciated. To all the members of the Morris Group my heart felt thanks for friendly assistance at many stages of the research.

Most of all, I would like to express my deepest gratitude to my parents for their support, financially and emotionally, during my years of education. And during the trying times of thesis research and writing the morale support given by Yvonne.

This work was supported by the Director, Office of Energy Research, Office of Basic Energy Sciences, Materials Sciences Division of the U.S. Department of Energy under Contract No. DE-AC03-76SF00098.

INTRODUCTION

High field superconductors are either compounds or alloys that at low temperature, usually 4.2K, can carry large currents with no power dissipation due to their zero resistance. The superconductive compound that will be used in wound magnets for fusion or accelerator applications of the future is Nb_3Sn. The current the material can carry depends on the conductor geometry and the processing it receives. The geometric factors are the amount of Nb_3Sn in the conductor and how it is distributed through the conductor. Once the geometry of the conductor is fixed the properties of the wire are determined by its processing. If no broken or irregular filaments are present then the heat treatment the wire receives ultimately determines its superconducting properties. The heat treatment influences the superconducting properties by altering the chemistry and microstructure of the Nb_3Sn.

Intermetallic compounds of Nb_3Sn are brittle and cannot be deformed into wire by common wire manufacturing methods. Special processes are required to fabricate them into conductors. The most common method used to produce multifilamentary conductors of Nb_3Sn is the "internal bronze" process [1,2,3,4]. Figure 1 is a schematic diagram of the fabrication process. Niobium rods are inserted into a Cu-Sn bronze billet which has been drilled with holes and is subsequently deformed by extrusion and drawing. This is then bundled and deformed to produce a high density of small filaments. The bundling is usually done to give a wire 2,000-10,000 filaments approximately five microns in diameter. The composite is then heat treated to form the Nb_3Sn at the Nb-bronze interface. During the drawing many anneals are required to prevent the bronze from cracking. This elaborate procedure results from the brit-

tleness of Nb_3Sn; it cannot be deformed by conventional methods, such as extrusion, swaging, and drawing, and therefore must be formed after deformation. Figure 2 is a micrograph of a cross section of a commercial "internal bronze" wire which has been deep etched to reveal its geometry. The center consists of the bronze and 2869 Nb filaments, separated from the external Cu stabilizer by a Ta barrier.

The "internal bronze" process is well suited for conventional wire fabrication methods. Large billets of Cu-Sn bronze can be made and deformed by extrusion, which produces long lengths of wires; making this aspect of the process economical. However, compared to other methods, the processing is labor and energy intensive due to the annealing steps, and the critical currents produced by this process appear to be too low for some potential applications. Accelerator magnets being designed at Lawrence Berkeley Labratory will require the superconducting wire to carry greater than 1000 Amp/mm^2. Conductors produced today by the internal bronze process can only carry 600 Amp/mm^2 (4.2K) before transforming to the normal state.

Two methods of increasing the critical current, I_c, under specified operating conditions of temperature and magnetic field, are possible. One is to increase the amount of Nb_3Sn in the cross section of the wire. The other is to improve the quality of the Nb_3Sn produced. The optimum bronze-to-niobium ratio in the "internal bronze" process is 3 for a bronze with about 7 atomic percent (a/o) Sn. At this ratio all of the Nb will be converted to Nb_3Sn. The "internal bronze" process, as a result, is limited by the maximum Sn solubility in Cu which is 7.8a/o, 13.5 weight percent (w/o). Above this tin concentration Cu-Sn intermetallic compounds form in the bronze rendering it unworkable to the extent required by the internal bronze process. As a result the volume fraction of Nb_3Sn can not be increased. Therefore, if the I_c of

the this process is to be increased the quality of the Nb_3Sn layer must be improved (i.e. the Nb_3Sn present must carry more current).

Many new fabrication techniques are being developed which are modifications of the "internal bronze" process. The techniques may differ slightly in internal geometry but the major distinction between them is the source of tin in each process. One technique, the external tin process, starts with a Cu-Nb composite which is deformed to final size, plated with tin, and heat treated to form the Nb_3Sn. The other method, the high tin process, starts with a Cu-Nb-Sn composite which is deformed to final size and heat treated. Figure 3 shows the three processes schematically, emphasizing the tin source in each process. These new methods have the advantage that no anneals are needed during processing because the copper is ductile. Also, these methods produce more Nb_3Sn because the tin supply is not limited by the maximum solubility of tin in copper. There is also some evidence which shows the quality of the Nb_3Sn produced in the high tin process may be better than that produced in the internal bronze process [5].

Certain superconducting properties are strongly influenced by metallurgical variations in the wire. The three basic parameters associated with every high field superconductor are the critical temperature, critical current density, and critical magnet field. The three dimensional surface in Figure 4 whose axes are temperature, critical current, and magnetic field, shows how the three parameters interact. Above the surface the material is in the normal state; below it is a superconductor. The critical temperature, T_c, and critical magnetic field, H_c2, are intrinsic to the material, and are affected by the composition, state of order, and strain. On the other hand, the critical current density J_c, is strongly affected by microstructure, primarily by grain size. The Nb_3Sn grain size formed by the internal

bronze process depends on the heat treatment temperature (as can be seen from Figure 5) and time at temperature.

All of the critical current testing in this work is done at the boiling point of liquid helium, 4.2K. Hence, the vertical section shown in Figure 4 is used to show the variation in J_c as a funtion of applied magnetic field H. The improvement of a material for application at 4.2K requires that this section be shifted to create a better characteristic $J_c(H)$.

Research of a commercial wire shown in Figure 2 [6] revealed that its high and low field properties vary differently with heat treatment (Fig. 6). A low aging temperature produces a higher J_c at low fields while a high temperature promotes high J_c at higher fields. Both of these phenomena can be explained by the microstructural and chemical state of the Nb_3Sn which forms during the heat treatment. The Nb_3Sn layer has three distinct shells, each of which has a distinct grain morphology. The inner shell contains columnar grains, the central shell consists of fine equiaxed grains, and the outer shell has large irregular grains. The volume fraction of each shell varies with heat treatment. From studies of the J_c variation with heat treatment it has been found that the central shell of the equiaxed fine-grained layer carries most of the current and the coarse, large-grained layer at the periphery of the filament carries little current. The outermost shell has the largest volume of the three shells, due to the cylindrical shape of the filaments, but carries little current. It has been shown that an optimized heat treatment schedule increases the volume fraction of the central fine-grained shell at the expense of the other two shells. Thus, it is believed that an increase in the I_c of the wire (J_c of the layer) will result if the grain size of the outermost shell is reduced.

The high field properties of the commercial wire can be explained

by the tin variation in the Nb_3Sn layer with heat treatment [6]. The variation of the Sn profile across the layer is seen in Figure 8 with high temperature aging promoting the smallest gradient near the stoichiometric value of 25 a/o. To obtain a high H_c2 the composition of the Nb_3Sn must be near 25 a/o Sn, though there is evidence that the highest H_c2 occurs at compositions slightly away from stoichiometry [7]. As can be seen in Figure 7, the high field J_c is increased due to the improved tin distribution in the layer.

Dopants have also been added to improve the J_c-H properties of the internal bronze process wire. These dopants are introduced into either the bronze or niobium before processing. The dopants improve the J_c-H properties of the wire by either altering the intrinsic properties of the Nb_3Sn or by improving the microstructure of the layer. The microstructure is improved by a reduction in grain size.

It has been shown that the critical current of a wire can be increased by either of two methods; increasing the Nb_3Sn content of a wire, or improving the Nb_3Sn quality. The goal of this reseach is to obtain a better fundamental understanding of the bronze process and to extend the previous work of improving the J_c of commercially processed internal bronze Nb_3Sn layer. From prior work on the layer structure of Nb_3Sn conductors an improvement in J_c may result if the grain size of the outer shell is reduced. Togano et. al. [8] and Tachikawa [9] have reported that the addition of Mg to the bronze of an internal bronze process monofilament would reduce the Nb_3Sn grain size. Therefore, this work was undertaken to determine the influence of magnesium on the grain size and morphology of the Nb_3Sn layer and the effect of magnesium on T_c, H_{c2}, and I_c and J_c.

To obtain better correlation to a commercial product a multifilamentary wire containing 133 filaments was produced. The multifilamen-

tary geometry was also chosen for two other reasons. The filaments produced by this process are less than 20 microns in diameter and small filaments are needed to prevent cracking of the Nb_3Sn layer. Also this filament size facilitates transmission electron microscopic observations. The production schedule for a laboratory scale multifilamentary conductor was determined. The effect of Mg on the processing parameters was also ascertained.

EXPERIMENTAL PROCEDURE

A. Bronze Tubing Manufacture.

Bronze ingots were fabricated by alloying high-purity, oxygen-free copper and high-purity tin in quartz ampoules evacuated and back filled with argon. The 500-700gm ingots which resulted were 25 to 27mm in diameter and 100mm in length. The best method for adding Mg was to drill a hole in the Cu and place Mg along with some Sn into the cavity. This starts alloying the Mg as the temperature is raised to the melting point of Cu. By controlling the maximum melt temperature, the time in the molten state, and the cooling rate of the material, the Mg-quartz reaction and chemical segregation on cooling can be minimized. The quality of the ingot was determined by measuring hardness along its length. If the Rockwell B hardness was between 60 to 70 along the entire length of the ingot, it was judged to be sound and the Sn distribution was found to be uniform in separate tests. The post homogenization hardness was about 30-40 (Table I).

The first ingots produced were homogenized at 750°C for 24 hours and form-rolled to about 50% reduction in area. The deformation was done at room temperature in two passes, 22.2mm(7/8 in.sq.) and 19.0(3/4 in.sq.), with a rolling speed of 178mm/s(35 ft/min.). The ingots were

again homogenized at 750°C for 24 hours. After homogenization the ingots were swaged at room temperature to 15.9mm(5/8 in.) rods and machined into three tubes with different dimensions, as required by the bundling sequence. One ingot supplied all of the tubing to produce a 133 filament wire. The three tubes by order in the bundling sequence had the following dimensions:

	O.D.		I.D.	
	mm	in.	mm	in.
Monofilament tube	11.4	0.450	6.35	0.250
7 filament tube	11.4	0.450	7.54	0.297
133 filament tube	12.4	0.490	8.13	0.320

The homogenization-rolling treatment was altered for the high Mg bronze ingots (>0.1 a/o). To prevent cracking during form-rolling the homogenization temperature was lowered to 700°C and the time was shortened to 12hrs. The reduction per pass was reduced, such that, the rolling was done in four passes. Further notes and observations on the bronze production can be found in the appendix.

B. Wire Processing.

The 133 filament wire was manufactured by a three-step bundling process. A single filament wire was produced by inserting a 6.35mm (0.250in.) Nb rod into a bronze tube and co-deforming the composite by swaging and drawing to 2.36mm (0.093in.). Seven of these single Nb core rods are consolidated in another tube which is swaged and drawn to 1.60mm (0.063in.). Nineteen of these seven-filament wires are combined in the last tube and deformed to 0.51mm (0.020in.).

C. Heat Treatment.

The wires were heat treated at five temperatures: 650, 700,

730,750, and 780°C for various times ranging from 1 to 20 days. The heat treatments were done in Linberg box furnaces with a temperature uncertainty of 5°C. The wires were encapsulated in quartz ampoules which were back-filled with argon so that, the internal pressure was approximately the ambient pressure (14.7psi) at the heat treatment temperature.

D. Metallography.

The wires were studied by optical and electron microscopy. A Zeiss Metallograph was employed for optical studies. Optical observations were used to determine the quality of the wire during processing. All area fraction determinations of the Nb_3Sn were done from scanning electron micrographs. The observations were done on an ISI scanning electron microscope (SEM) operating at 25kV with a working distance of 20mm. To uniformly etch the sample revealing the A15 for obsevation the following solution was used: 9% water (H_2O), 9% concentrated sulfuric acid (H_2SO_4), 9% hydrofluoric acid (40-48% HF by vol.), 1% hydrogen peroxide (30% H_2O_2 by vol.), and 72% lactic acid.

Qualitative Nb_3Sn grain size results were obtained by fracturing the wires and observing the fracture surface of the Nb_3Sn layer. The best fracture surface resulted if the wires were cooled to liquid nitrogen temperature before fracturing. The fracturing was done by hand with pliers at a point where some of the bronze was removed by a concentrated nitric acid solution.

E. Nb_3Sn Composition.

The chemical composition of the Nb_3Sn layer was determined by an electron microprobe (EMP) operating at 15kV, which was equipped with a wave length dispersive spectrometer.

F. Critical Temperature Measurements.

The critical temperature was measured inductively on samples which

had been coiled into a loop with a diameter of 6.3mm and heat treated. The bronze was removed with a nitric acid solution to prevent shielding effects. The measuring device had a ripple frequency of 10kHz. and a 1 gauss amplitude.

G. Critical Current Measurements.

The critical current (I_c) was measured by a four-point probe technique. The tests were done at 4.2K in solenoidal magnets at the Francis Bitter National Magnet Laboratory. The magnetic field was fixed and the current was ramped. The short samples were 3 cm in length with the voltage taps placed in the center 5mm apart. A fixed criterion of 2 microvolts between the taps was used to locate the transition. Obtaining reliable and reproducible data for I_c determination is not a simple task. The interpretion of the data depends on the testing geometry and the criteria used to to obtain the I_c values. The paper by Goodrich and Fickett [10] is a excellent source for methods of I_c data collection and interpretation.

The critical current densities (J_c,I_{cNb}) were determined by dividing the critical current by the areas of Nb_3Sn and Nb in the wire cross-section respectively. The areas were measured from SEM micrographs with a CALCOMP 9000 SERIES digitizer.

RESULTS

A. Wire Fabrication.

Sample micrographs of the five wires produced in this work are seen in Figures 9a,b. A micrograph of a deep etched low-tin, Mg-free wire which has been heat treated for 2 days at 730°C is seen in Figure 10. The unreacted Nb core is visible in the center of each filament. All of the wires except one have a bronze to niobium ratio between 10

and 15. The high-tin, Mg-free wire has a ratio of about 25 to 1 (Fig. 9a).

The Nb filaments in the central bundles retained their cylindrical shape, while those at the wire perimeter have a ribbon or tape nature. Qualitatively the wires in Figures 9a,b do not appear to have the same proportion of ribbon-to-rod shape filaments. The curvature of the filaments affects the layer structure which forms during heat treatment High curvature, promotes a small grain structure. Low curvature in a tape promotes a large grain structure. This may be a factor to consider when interpreting the critical current results.

Many annealing treatments at 450°C are required to prevent cracking of the bronze. The wires did not have a fixed reduction-in-area-anneal schedule. The Mg-free wires required the fewest anneals due to their good ductility which permitted 50-80% reduction in area between anneals. The Mg-bronze wire with 0.62 a/o Mg could be swaged only 15-20% before annealing was required. As the deformation progressed larger reductions of 40-50% by drawing were achieved.

Filament breakage was encountered in the Mg-bronze wires. The breakage occurred in the later stages of drawing the 133 filament wire. Figure 11 shows two micrographs of the low-tin wire with 0.10 a/o Mg at two stages of the final drawing process. No broken or large irregular shaped filaments are observed at a wire diameter of 2.64mm (0.104in.). When this wire is viewed laterally (after the bronze has been removed by etching) slight modulations in the filament diameter are seen (Fig. 12). When the same wire is viewed laterally at the 1.02mm (0.040in.). stage, random broken filaments and large modulations along the filaments are observed (Figs. 13,14). It appears that some of the breakage may have been due to inclusions in the wire (Figs. 15,16). Energy dispersive x-ray analysis (EDS) of the inclusions reveals only Nb; Mg

and Sn could not be resolved from the background. It was not possible to determine if the inclusions were in the starting material or if during processing a reaction occurred forming the particles. When a 0.62 a/o Mg wire was produced with the new schedule no broken filaments were oberved. The breakage seems to have two sources, one associated with a "Rayleigh type" instability and the other resulting from inclusions in the wire.

The broken filaments occurred at particular regions in the wire. The wire cross section has one bundle of seven filaments in the center surrounded by six bundles in the first shell, in turn surrounded by twelve bundles in the outer shell. All of the broken filaments occurred in the center bundle or the first shell.

B. Nb_3Sn LAYER FORMATION.

The Nb_3Sn layer formed at different rates in different wires. As can be seen from the plot of Nb_3Sn area versus reaction time for the low-tin wires, the Mg-free material has a smaller slope. (Fig. 17) The layer growth exponent, n, in the equation $d=kt^n$ where d is the layer thickness was obtained from the slope of a log-log plot. The low-tin Mg-free wire has a layer growth exponent of about 0.5. This correlates well with previous work by Suenaga [3]. The high-Mg wire, on the other hand, had an exponent of about 1.0. These values were determined from the 650 and 700°C aging curves. The only value which can be obtained from the high-tin wires is an exponent of 0.70 for the Mg-free wire heat treated at 650°C. The other wires were too near complete reaction. The positive deviation of the exponent for the high tin wire correlates with previous work by [3]. As can be seen in Figure 17, for a fixed time the wires will have different volume fractions of Nb_3Sn; as a result time is an inadequate parameter for comparison of J_c and I_{cNb}.

C. Critical Current Density.

From a research perspective the current that the Nb_3Sn layer can carry is important. It permits a comparison of wires with different Nb contents and various bronze compositions by the quality of the Nb_3Sn in each wire. Therefore, two normalization procedures were used to compare the different wires. One was the the standard critical current density, J_c, which is the I_c divided by the Nb_3Sn area in the wire cross section. The other, the normalized critical current, I_{cNb}, is calculated from the initial Nb area of each wire. The normalized critical current accounts for the different amounts of Nb in each wire.

Each normalization method has its own merit. The critical current density J_c, is a better normalization for comparisons at all reaction times, but due to the difficulty of determining the Nb_3Sn area J_c is a very laborious value to obtain. The normalized critical current, on the other hand, requires only a few area calculations for each wire, but for comparison between the wires at short aging time this measure is not adequate. Near complete reaction the two methods are very similar.

Representative I_{cNb} heat treatment curves are seen in Figures 18. The figure shows variation in I_{cNb} as a function of heat treatment time for the low-tin Mg-free wire studied. The curves have a shape similar to age hardening curves; I_{cNb} increases with time, reaches a peak at an intermediate aging temperature, and overages at high temperature in a short time with a peak lower than the intermediate temperature.

Figure 19 shows the J_c versus aging time for the same wire plotted in Figure 18. The curves have a similar shape but the heat treatment curves for 650 and 700°C now have peaks due to the incremental increase in I_c not offsetting the incremental increase in the Nb_3Sn area. The curves are similar at high temperature or long aging time when the

filaments are near complete reaction.

Since the wires reacted at different rates an equitable method to compare the wires is by plotting J_c or I_{cNb} versus percent of Nb filament conversion to Nb_3Sn. Figures 20a,b,c,d are for I_{cNb} and Figures 21a,b,c,d are for J_c. The letter index a,b are for the 6.7 a/o Sn wires and c,d are for the 7.8 a/o Sn wires. It is seen that the 0.62a/o Mg addition to the low tin wire improves its J_c and I_{cNb} at 650, 700 and 780°C (Figs. 20a,21a). For the aging temperatures 730°C and 750°C the Mg-free wire has superior J_c and I_{cNb} for early stages of the heat treatment. However, near complete reaction the 0.62 a/o Mg wire is better (Figs. 20b,21b). At 750°C there is little overlap in the percent reaction due to the faster layer growth rate in the Mg doped wire. Nevertheless, from a short extrapolation it can be inferred that Mg has a significant effect.

Figure 22 shows that 0.62 a/o Mg increases the J_c for all heat treatment temperatures when compared at certain stages of the reaction. The temperatures 650, 700, 730, 750, and 780°C were compared at 62, 85, 80, 90, and 95 percent completion respectively. The optimum aging temperature is in the range 700-730°C for all wires when similar stages of the reaction are compared.

The high tin content wires present an interesting result. When aged at 650 or 700°C the Mg-free wire has a better J_c, Figure 20c, and I_{cNb}, Figure 21c, but for aging temperatures of 750 and 780°C the 0.10 a/o Mg wire is superior Figures 20d, 21d. At 730°C aging the two curves cross at about 95% filament conversion. This result suggests that filament size influences the layer structure more than the 0.10 a/o Mg addition at low aging temperature, while at high temperatures the 0.10 a/o Mg wire is superior due to the reduced coarsening rate.

The critical current density of the 0.62a/o Mg-doped wire is 100-

150% greater than the Mg-free wires at all fields when compared near complete reaction. Representative curves for a few heat treatment conditions are seen in Figure 23. Each reaction temperature has the same filament conversion, 650°C is 62%, 750°C is 90%, and 780°C is 85%. The curves have a form similar to the commercial wire previously studied. The low aging temperature 650°C is better at low field, while the high temperatures, 750 and 780°C, are better at high field. The only exception to this is the low-tin, Mg-free wire heat treated at 780°C.

Microstructural studies by SEM show that the grain size of the Nb_3Sn layer for wires heat treated at 780°C is much smaller with a 0.10 and 0.62 a/o Mg addition (Fig. 24). The layer is uniform with no columnar grain shell near the unreacted Nb core or large grain shell at the filament periphery. The results at lower aging temperatures are inconclusive and must be resolved by TEM.

It was determined by EMP analysis that during heat treatment most of the Mg in the bronze diffuses to the Nb_3Sn layer (Figs. 25,26). The Mg concentration in the Nb_3Sn layer is about 3-4 a/o Mg. To determine if the Mg is segregating to the Nb_3Sn grain boundaries Auger analyses of the boundaries were done but the results are inconclusive. A definite cause for the increase in J_c and I_{cNb} at high fields can not be given, only inferred.

C. Critical Temperature

The critical temperatures of the 0.62a/o Mg and Mg-free wires were measured for several aging conditions. The peak critical temperature of the wire is not altered by Mg addition. The critical temperature reaches its optimum value of about 18K after 48 hrs. at 700°C. The 0.62 a/o Mg wire has a lower critical temperature for shorter aging times, but it peaks at the same value as the Mg-free material (Table

II). The width of the transition decreases with aging time. However, the Mg-bronze material has a width about twice that of the undoped wires at optimum aging. The difference in the transition width increases with aging time.

DISCUSSION

A. Wire Fabrication.

The broken filaments appear to have two causes, inclusions in the material and filament instabilities. The exact source of the inclusions is not known. EDS analyses found no tin, copper, or magnesium in the inclusions; niobium was the only element detected. This suggests the inclusions are probably niobium oxide particles that were in the rod initially or formed during processing. Since the niobium rod was completely consumed in wire fabrication, a study of the bronze was performed to determine whether the inclusions could have formed during processing.

As can be seen in Table I the oxygen concentration in the Mg bronze is less than that in the Mg-free bronze. Assuming Mg has no catalytic effect on oxide formation in the Cu-Nb system, one would expect oxides to form in the Mg-free bronze instead. But no inclusions are observed in the Mg-free wire. Therefore, the source of the inclusions seems to be the niobium rod itself. Since the niobium is a high purity electron beam melted rod the inclusions must have originated on the surface of the rod. Before bundling as a monofilament the niobium rods were swaged to size and cleaned in an acid solution. The acid cleaning should be altered to deeply etch the niobium surface, thus removing all the inclusions.

The filament instability has two sources, one thermal the other

mechanical. The thermal instability is of the Rayleigh type. The cylindrical shape is unstable; it is energetically favorable for the cylindrical rod of material to break-up into a row of distinct spherical particles. From a simple model which assumes a sinusoidal modulation of the rod surface, and transport of material by interface diffusion it is found that the modulation wave length is approximately 4 times the filament diameter. The oscillations observed in Figure 12 are about twice the diameter. For such a crude model the values are relatively close; however the result may be fortuitous rather than significant.

The slight oscillation in the filament diameter could be the precursor of filament breakage by a mechanical instability. Due to the reduced cross sectional area of the filament at the low points of the modulation one would expect these regions to be the first to "neck". Figure 13 reveals modulations along a filament which has appeared to "neck" periodically. However, there are some inclusions around this region making the exact mechanism unclear.

B. Nb_3Sn LAYER FORMATION.

The layer growth exponent is increased by about a factor of two with the addition of 0.62a/o Mg to the bronze matrix; this implies a change in the layer growth mechanism. Other researchers have found that tin diffusion through the Nb_3Sn layer controls the growth of the layer when the tin concentration in the bronze is below 6.8a/o.

No cracks are observed in the Nb_3Sn layer for any of the wires studied, so another source of the variation in the layer growth exponent must be found. It appears high Mg concentrations in the layer are required to alter the exponent since most of the Mg in the bronze well be incorporated into the Nb_3Sn layer (Figs. 25,26). Togano et. al. [8] and Tachikawa [9] studied monofilaments which had 0.5a/o Mg addition

to the bronze, but their bronze-to-niobium ratio was only 3, much lower than this work. As a result, they never obtained the high Mg concentration in the Nb_3Sn layer and subsequently observed no exponent variation.

Electron microprobe analyses of the Nb_3Sn layer in a seven filament wire with a 0.62a/o Mg bronze show a distinct Mg gradient across the layer with the Mg accumulation at the Nb_3Sn-bronze interface (Fig. 26). The 133 filament wire, however, shows no substantial Mg gradient across the layer. The small filaments in the 133 wire make sample preperation for EMP difficult. The drop in the Mg concentration at the Nb_3Sn-bronze interface is probably not characteristic of the material. The drop in concentration can probably be attributed instead to rounding of the filament surface when the wire was polished. Scanning electron microscope observations made by Suenaga [11] of the 6.7a/o Sn with 0.62a/o Mg heat treated at 750°C for 2 days reveal some particles in the Nb_3Sn layer near the Nb_3Sn-bronze interface. The exact nature of this reaction of the rate is uncertain.

C. Superconducting Properties.

The results show that the optimum aging temperature for a high J_c at 10 Tesla is in the range 700-730°C for all the wires, even though they have different bronze compositions and different filament diameters. Other researchers have found this to be the optimum temperature range for wires with different compositions and geometries; Suenaga [3] found 725°C to be the optimum aging temperature after an extensive literature search. The grain size (Fig. 5) and layer structure do vary with the internal geometry and bronze composition of the conductor but peak properties occur for heat treatments at 700-730°C. This important result implies that the optimum aging temperature for all "bronze-type" processes should be in the temperature range 700-730°C. The results of

Togano et. al. [8] are somewhat misleading in the form initially presented (Fig. 27). Figure 27 is a graph of I_c variation with aging temperature for a fixed aging time of 100 hours. It gives the impression that the optimum in I_c occurs at about 800°C. When one uses their published layer thickness results and calculates the J_c values, Figure 28 is obtained. The peak is shifted to less than 750°C. This correlates well with this work. The results of this study are presented in a similar manner in Figure 28. There are two points to notice in these two figures. One is the quality of the Nb_3Sn layer produced in each wire. The two materials have comparable J_c values but at different fields, 10T this work and 6.5T Tongano's. Therefore, the Nb_3Sn layer of this work has a better layer microstructure. The other point is the inadequacy of an isochronal graph format for comparisons of wires with different bronze compositions. The reaction time was fixed at all temperatures; as a result, the wires with different volume fractions of Nb_3Sn are compared. At high aging temperatures no improvement in J_c is observed. However, comparison of the different wires at similar stages of the reaction reveals a substantial improvement for heat treatment temperatures of 750°C or greater (Figs. 20,21).

The increase in J_c at low field is will correlated with the observed microstructure. Sample micrographs of the three low-tin wires which have been heat treated at 780°C for 1 day are seen in Figure 24. The wires with 0.10 and 0.62a/o Mg added to the bronze have a uniform fine-grained Nb_3Sn layer. The Mg-doped wires do not have any columnar grains in the layer, while the Mg-free wire has elongated grains.

The variation in J_c with aging temperature and time is similar to that in previously studied internal bronze process wires [6]. Figure 6 is the $J_c(H)$ curves for a commercial internal bronze; wire Figure 23 is for this work. Both studies show the same trend; low aging tempera-

tures produce a high J_c at low fields, while high aging temperatures produce a high J_c at high fields. Preliminary microchemical results from scanning transmission microscopy (STEM/EDS) of the wires in this study [12] show the tin profiles to be similar to those in the commercial wire (Fig. 8). The STEM/EDS results also suggest the tin profile in the Mg-doped wire has a smaller gradient across the layer [12]. Some of the H_{c2} improvement may be attributed to this. The presence of magnesium, either distributed in the bulk or localized at the grain boundaries, will change the normal state resistance of the material and alter H_{c2} [7]. There is also some evidence that dopants in Nb_3Sn can prevent a low temperature martensitic transformation from occurring at about 40K. Suppressing the transformation increases H_{c2} [3]. In addition, the J_c of Nb_3Sn is very sensitive to strain at high fields. For the present, the increase in high field properties cannot be attributed entirely to the addition of magnesium.

SUMMARY AND CONCLUSIONS

1. A 10-15 microns filament multifilamentary wire can be produced in the laboratory by swaging and drawing. Processing parameters must be carefully controlled to prevent filament breakage.
2. Wires with 6.7 to 7.8 a/o Sn can be fabricated with up to 0.62 a/o Mg added to the bronze matrix.
3. Magnesium is readily incorporated into the Nb_3Sn layer during the heat treatment; there is little residual in the bronze matrix. The superconducting critical temperature of the 0.62 a/o Mg wire is only slightly altered from the Mg-free wire.
4. The optimum aging temperature to maximize the 10 Tesla critical current density for all the wires, i.e., at all compositions, is in

the range 700-750°C. All "bronze type" processes have this temperature range as their optimum. This uniformity implies that an intrinsic mechanism controls the Nb_3Sn layer formation.

5. The critical current of the low-tin 0.62 a/o Mg wire is superior to the Mg-free wire at all fields when the wires are compared near complete filament conversion to Nb_3Sn. For low aging temperatures a uniform increase in the critical current is obtained at all fields, while for high aging temperatures a greater improvement is obtained at high fields.
6. A 0.62 a/o Mg addition to the bronze matrix appears to alter the mechanism of Nb_3Sn layer growth. The layer growth exponent increases by about a factor of two with the 0.62 a/o Mg addition.

REFERENCES

1. A.R. Kaufmann and J.J. Pickett, Bull. Am. Phys. Soc., 15, 833 (1920).
2. E. W. Howlett, U.S. Pat. 3,728,165 (filed 10/19/1970); Great Britain Pat. 52,623/69 (filed 10/17/69).
3. M. Suenaga, Metallurgy of Continuous Filamentary A15 Superconductors, **Superconductor Materials Science**, Plenum Press, 1981, p. 20.
4. M. Suenaga and A.F. Clark (eds.), **Filamentary A15 Superconductors**, Plenum Press, 1980.
5. Cogan et al., IEEE MAG 17, 1981.
6. I.W. Wu, D.R. Dietderich, J.T. Holthuis, M. Hong, W.V. Hassenzahl and J.W. Morris, Jr., J. Appl. Physics, to be published.
7. T.A. Orlando, et al., **Proceedings 1980 Applied Superconductivity**, IEEE Trans. MAG 17, p. 368, 1981.
8. K. Togano, Y. Asano and K. Tachikawa, J. Less Common Metals, 68, 15, 1979.
9. K. Tachikawa, **Advances in Cryogenic Engineering**, ICMC vol. 26, Plenum Press, 1980.
10. L.F. Goodrich and F.K. Fickett, Cryogenics, May, 1982, p. 225.
11. M. Suenaga, private communication.
12. I.W. Wu, D.R. Dietderich, J.T. Holthuis, W.V. Hassenzahl and J.W. Morris, Jr., **Proceedings of Applied Superconductivity Conference**, IEEE MAG 19, 1982.

.FI TABLE1

TABLE I. Rockwell B Hardness Tests of Bronze Ingots Containing 11.6 w/o Sn according to the Magnesium Content.

		Mg CONTENT			
	w/o (a/o)	0.00 (0.00)	0.03 (0.10)	0.12 (0.35)	0.22 (0.62)
OXYGEN (a/o)		0.042	0.013	0.013	0.013
OXYGEN (w/o)		0.010	0.003	0.003	0.003
450°C/1 hr.		62.2	58.2	72.1	83.7
750°C/12 hrs.		44.5	36.9	38.5	38.6
750°C/12 hrs. + 450°C/2 hrs.		43.1	36.2	42.8	57.5

TABLE II. Critical Temperature (T_c) According to Magnesium Content of the Wire According to Heat Treatment.

Wire Composition and Heat Treatment	T_C(K)	ΔT_C(K)
6.7 a/o Sn + 0.0 a/o Mg		
700°C/0.5 Days	17.6	1.2
'' / 1 Day	17.8	1.6
'' / 2 Days	17.8	0.7
6.7 a/o Sn + 0.62 a/o Mg		
700°C/0.5 Days	17.2	1.6
'' / 1 Day	17.6	2.0
'' / 2 Days	17.8	1.3

FIGURE CAPTIONS

1. A schematic of the internal bronze process fabrication technique.
2. Micrograph of an Airco internal bronze commercial wire.
3. Three bronze type processes and how they supply the tin.
4. Nb_3Sn grain size variation with heat treatment temperature.
5. The critical surface in J-H-T space which bounds the normal and superconducting states.
6. $J_c(H)$ variation with heat treatment (Wu et al.).
7. Schematic of grain structure and tin profile across Nb_3Sn layer for commercial internal bronze wire.
8. Tin profiles across Nb_3Sn layer (Wu et al.).
9. (a) Micrograph of 6.7 a/o Sn wires.
   (b) Micrograph of 7.8 a/o Sn wires.
10. LBL internal bronze wire with 133 filaments that has been heat treated at 730°C for 1 day. The bronze has been removed with a deep etch.
11. Filament breakage in 133 filament wire at 0.20 in diameter and no broken filaments at 0.104 in. diameter.
12. Modulation in filaments at 0.104 in. wire diameter.
13. Modulation and inclusions in filaments.
14. Terminated filament.
15. Inclusions in filaments at 0.104 in. diameter.
16. Inclusion in 0.040 in. diameter wire that was analyzed by EDS. Only Nb was detected.
17. Plot of cross-sectional area of Nb_3Sn in wires versus aging time.
18. Normalized critical current (4.2K, 10T) at fixed temperature

versus aging time.

19. Normalized critical current density (4.2K, 10T) at fixed temperature versus aging time.

20. (a) I_cNb (4.2K, 10T) versus percent of Nb_3Sn formed in bronze wires (6.7 a/o Sn) heat treated at 650, 700 and 780°C.

    (b) I_cNb (4.2K, 10T) versus percent of Nb_3Sn formed in bronze wires (6.7 a/o Sn) heat treated at 730 and 750°C.

    (c) I_cNb (4.2K, 10T) versus percent of Nb_3Sn formed in bronze wires (7.8 a/o Sn) heat treated at 650, 700 and 780 °C.

    (d) I_cNb (4.2K, 10T) versus percent of Nb_3Sn formed in bronze wires (7.8 a/o Sn) heat treated at 730 and 750°C.

21. (a) J_c (4.2K, 10T) versus percent of Nb_3Sn formed in bronze wires (6.7 a/o Sn) heat treated at 650, 700 and 780°C.

    (b) J_c (4.2K, 10T) versus percent of Nb_3Sn formed in bronze wires (6.7 a/o Sn) heat treated at 730 and 750 °C.

    (c) J_c (4.2K, 10T) versus percent of Nb_3Sn formed in bronze wires (7.8 a/o Sn) heat treated at 650, 700 and 780 °C.

    (d) J_c (4.2K, 10T) versus percent of Nb_3Sn formed in bronze wires (7.8 a/o Sn) heat treated at 730 and 750°C.

22. J_c (4.2K, 10T) versus aging temperatures for wires compared at fixed percentages of Nb_3Sn.

23. J_c versus magnetic field for low-tin wires with 0.62 a/o Mg and 0.0 a/o Mg.

24. Fracture surface of low-tin wires heat treated at 780°C for 1 day.

25. Magnesium composition across Nb_3Sn layer in the 133 filament wire.

26. Magnesium composition across Nb_3Sn layer in the 7 filament wire.

27. The I_c (4.2K, 6.5T) versus aging temperature for an aging time of 100 hrs. (Togano et al.)

28. Critical current density of this work plotted with those of Togano. The plot shows the variation in J_c with aging temperature.

INTERNAL BRONZE PROCESS

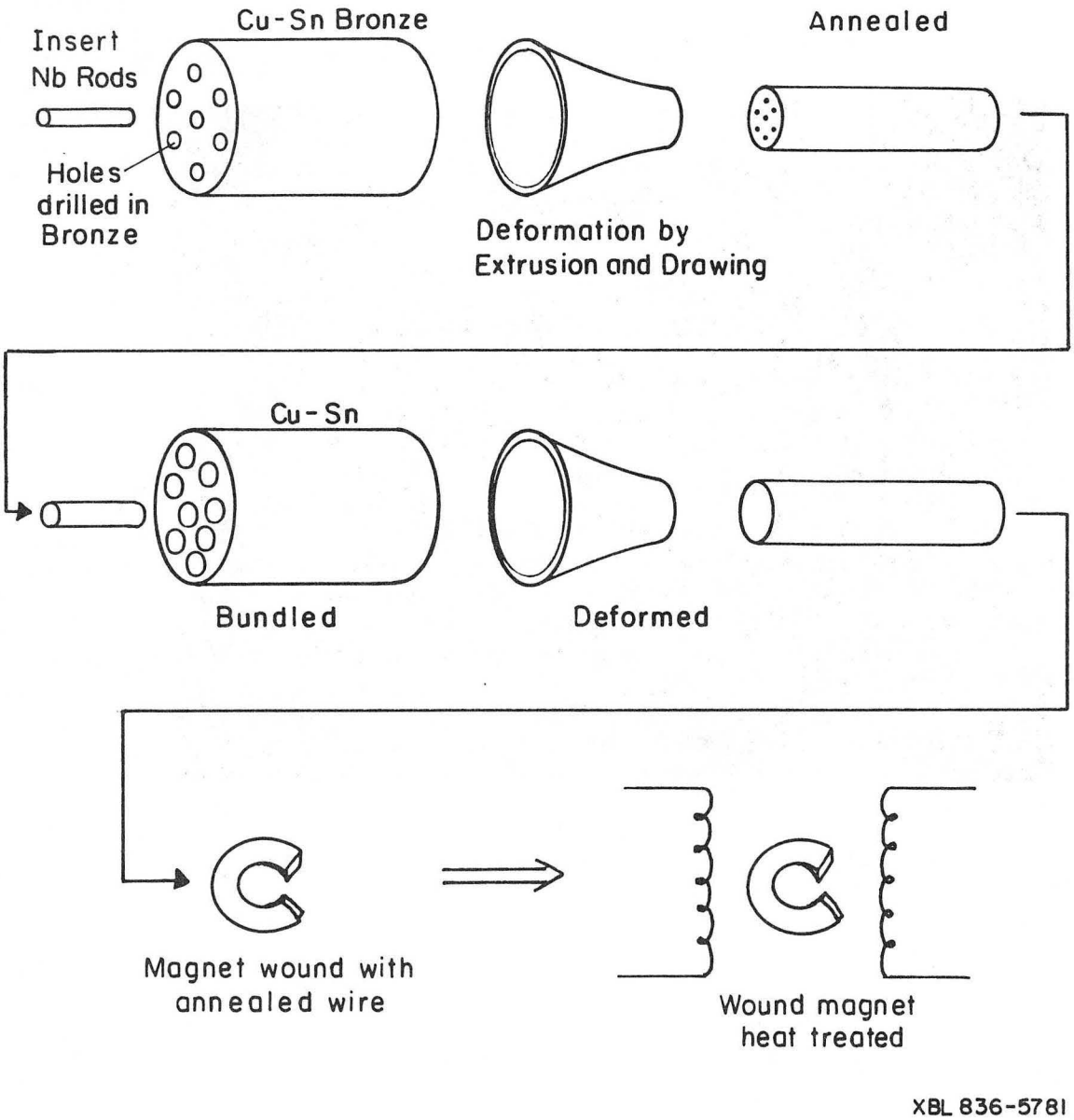

Fig. 1

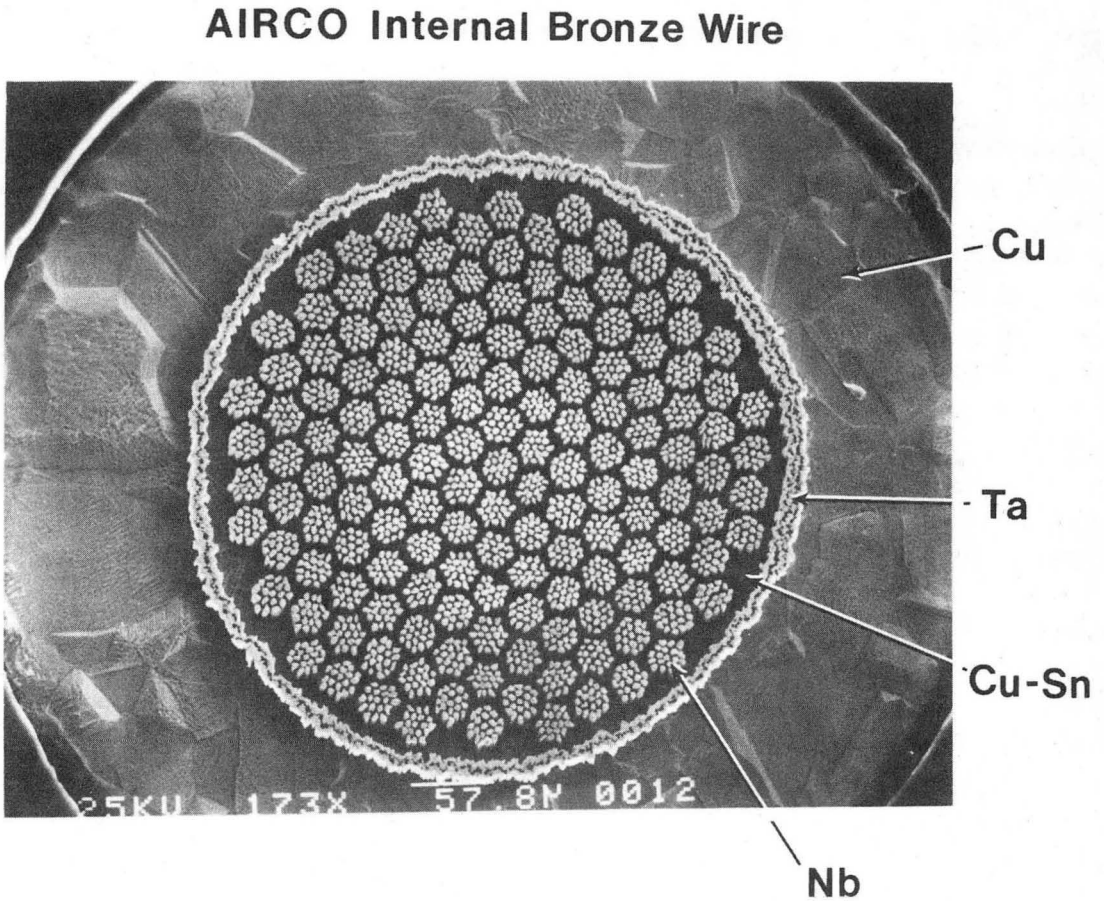

XBB 831-546A

Fig. 2

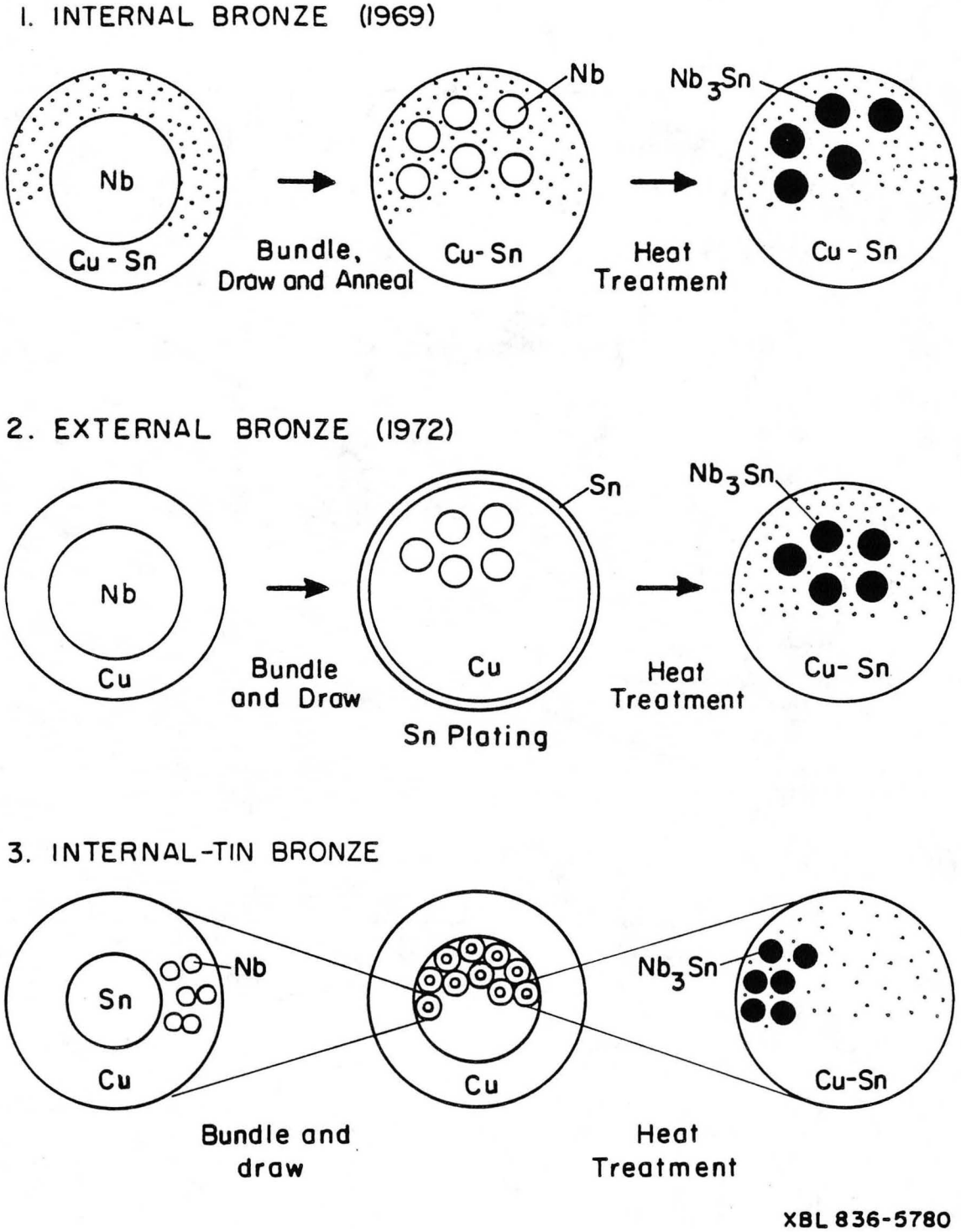
1. INTERNAL BRONZE (1969)
Nb
Cu - Sn
Bundle,
Draw and Anneal
Nb
Cu-Sn
Nb3Sn
Heat
Treatment
Cu - Sn
2. EXTERNAL BRONZE (1972)
Nb
Cu
Bundle
and Draw
Sn
Cu
Sn Plating
Nb3Sn
Heat
Treatment
Cu- Sn
3. INTERNAL-TIN BRONZE
Sn
Cu
Nb
Bundle and
draw
Cu
Nb3Sn
Heat
Treatment
Cu-Sn
XBL 836-5780

Fig. 3

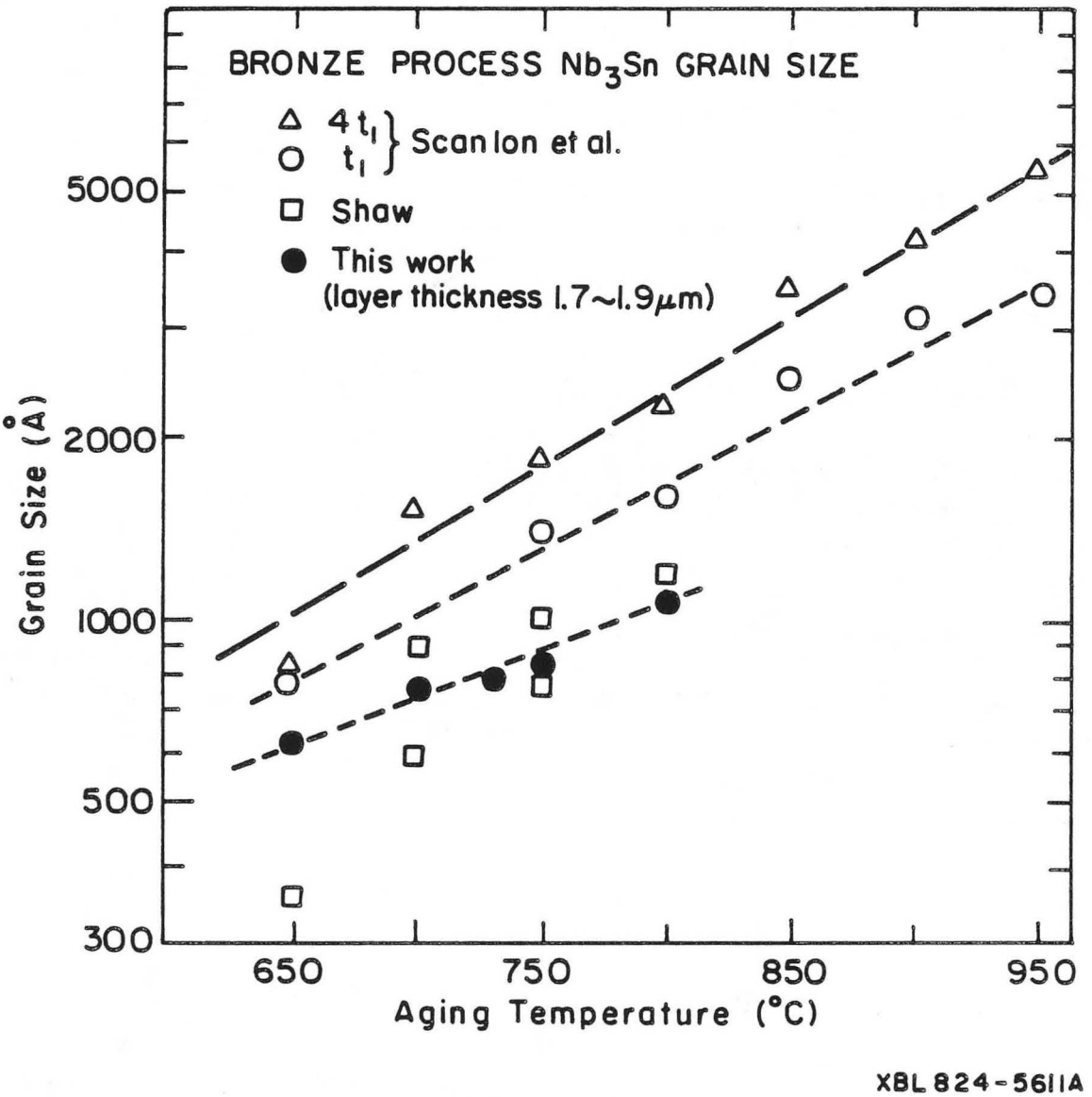
BRONZE PROCESS Nb_3Sn GRAIN SIZE
$4t_1$
t_1
Scanlon et al.
Shaw
This work
(layer thickness 1.7~1.9μm)
Grain Size (Å)
5000
2000
1000
500
300
650
750
850
950
Aging Temperature (°C)
XBL 824-5611A

Fig. 4

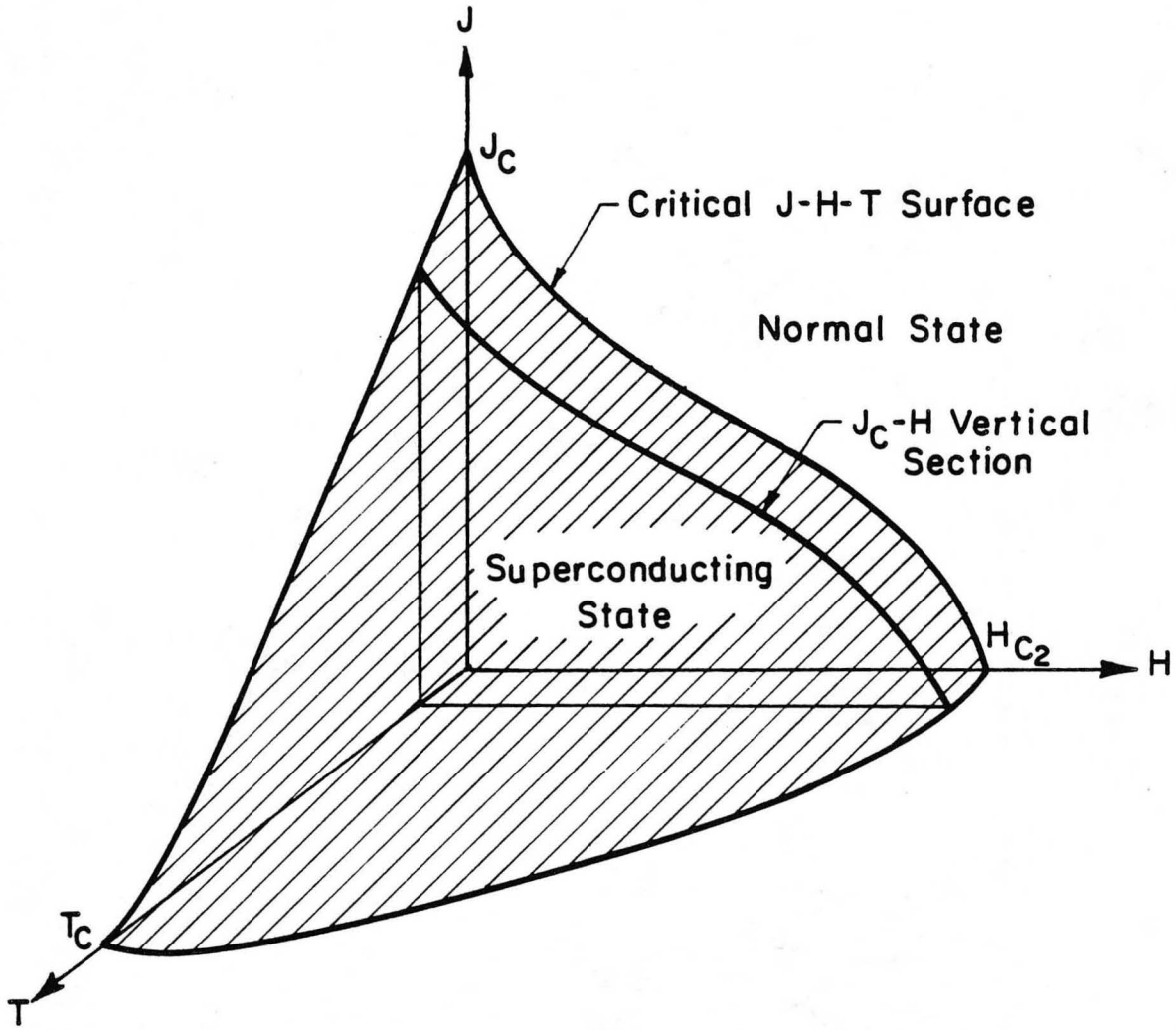
J
J_C
Critical J-H-T Surface
Normal State
J_C-H Vertical Section
Superconducting State
H_{C_2}
H
T_C
T
XBL 836-5778

Fig. 5

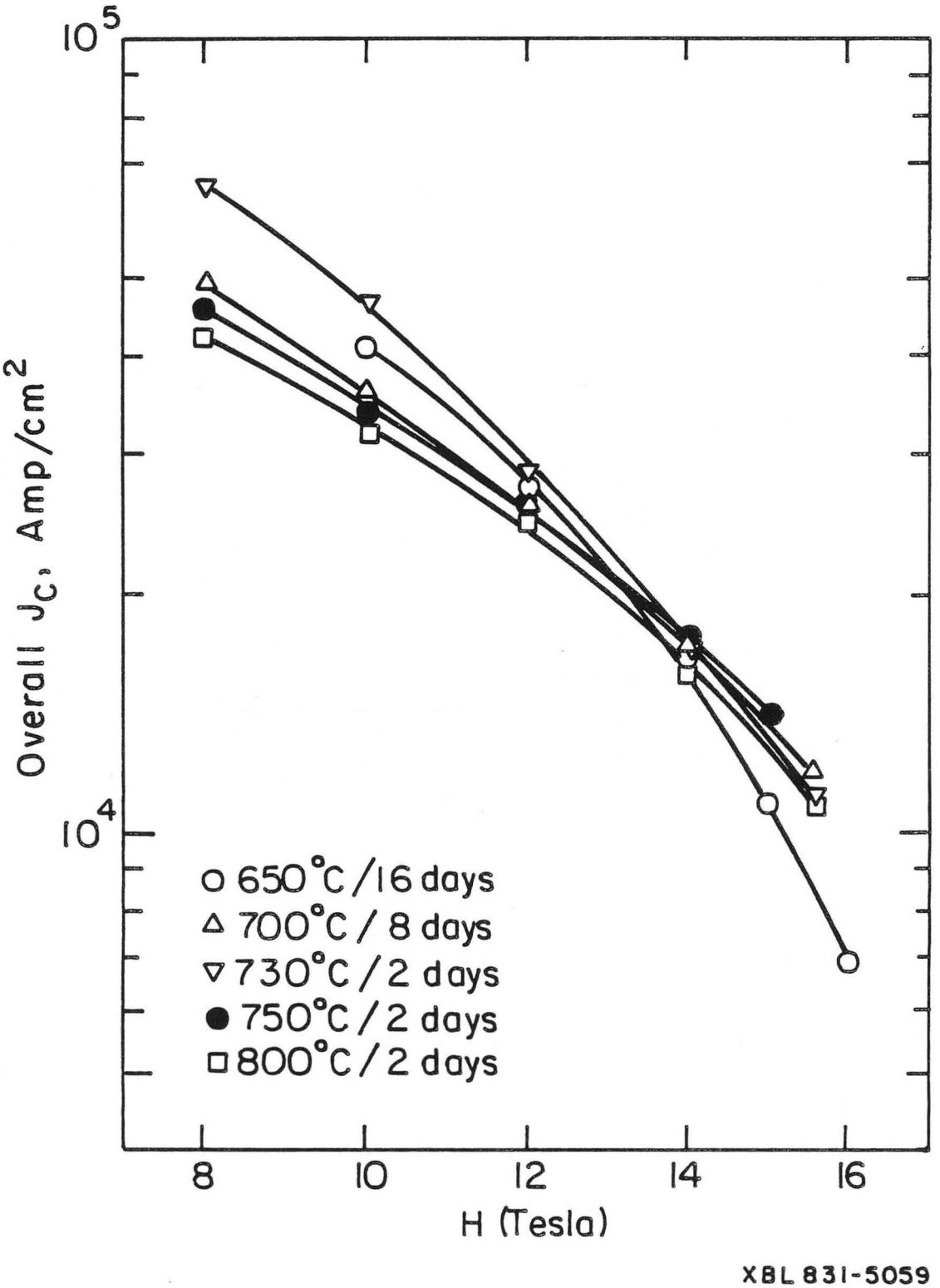
10^5
10^4
Overall J_c, Amp/cm^2
○ 650°C / 16 days
△ 700°C / 8 days
▽ 730°C / 2 days
● 750°C / 2 days
□ 800°C / 2 days
8
10
12
14
16
H (Tesla)
XBL 831-5059

Fig. 6

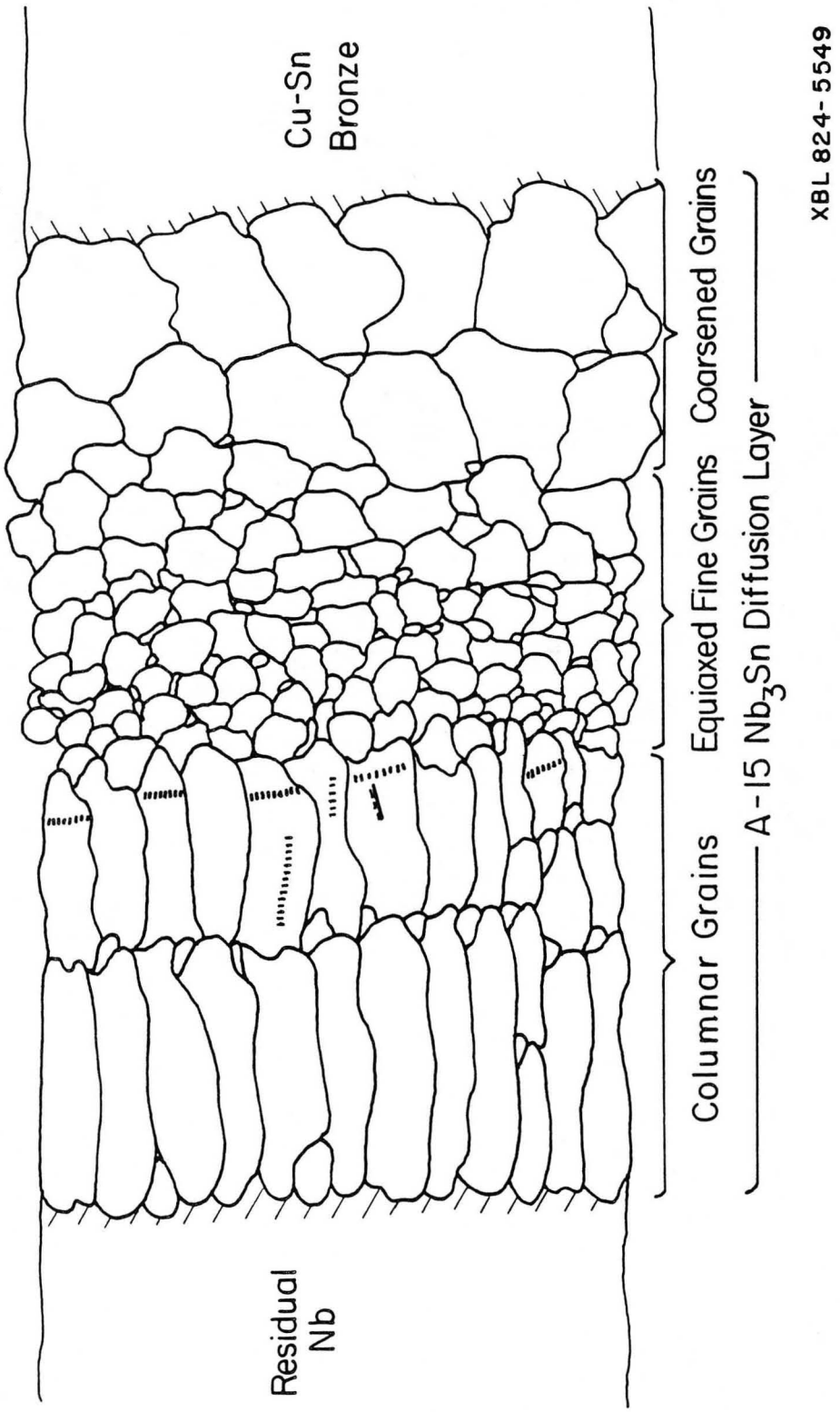
Cu-Sn
Bronze
Residual
Nb
Columnar Grains
Equiaxed Fine Grains
Coarsened Grains
A-15 Nb_3Sn Diffusion Layer
XBL 824-5549

Fig. 7

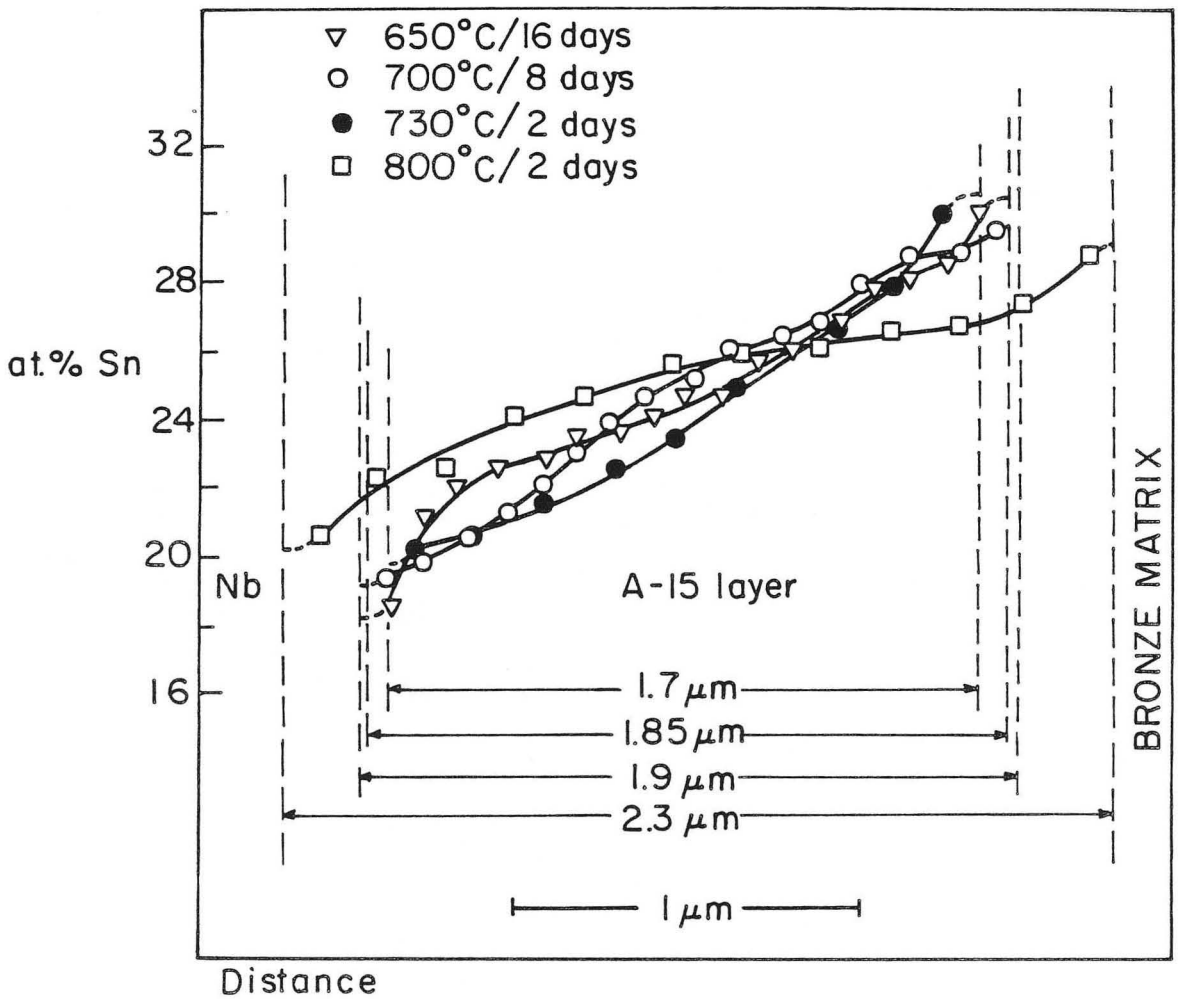
650°C/16 days
700°C/8 days
730°C/2 days
800°C/2 days
32
28
24
20
16
at.% Sn
Nb
A-15 layer
BRONZE MATRIX
1.7 μm
1.85 μm
1.9 μm
2.3 μm
1 μm
Distance
XBL 831-5054

Fig. 8

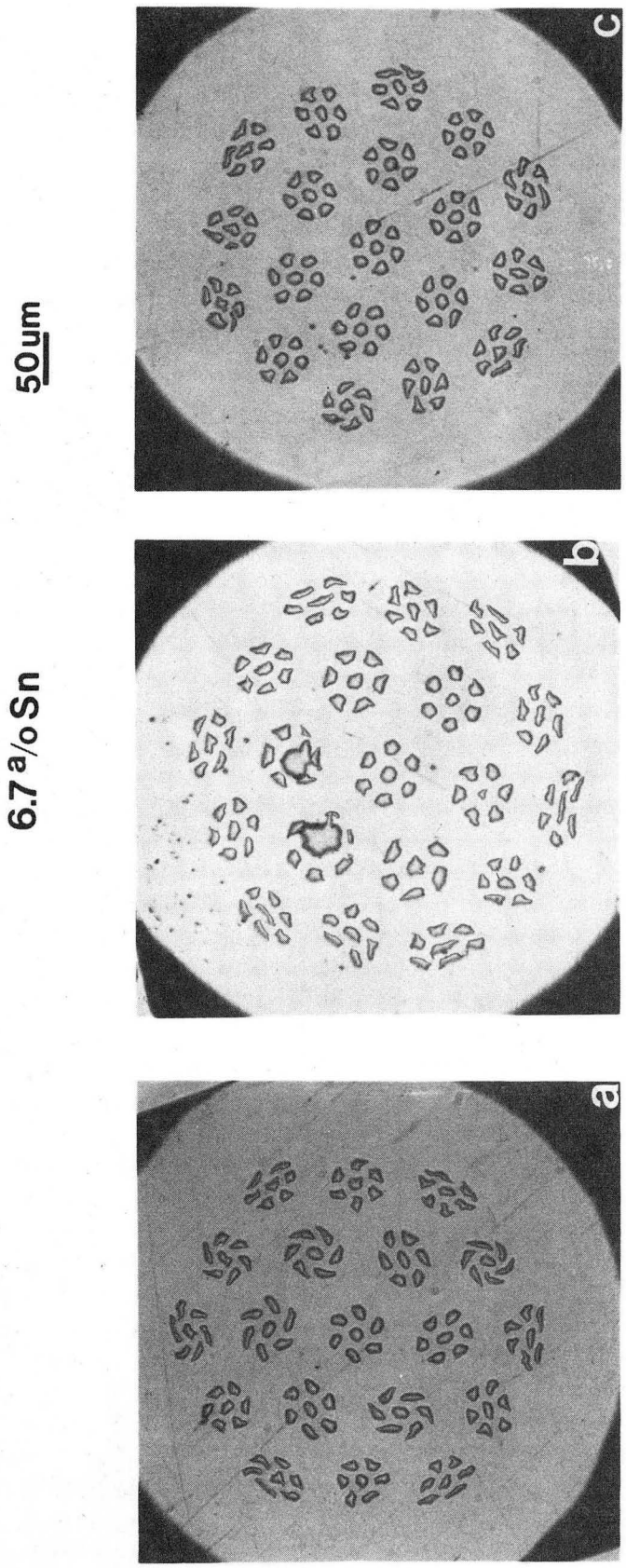

XBB 836-5035

Fig. 9a

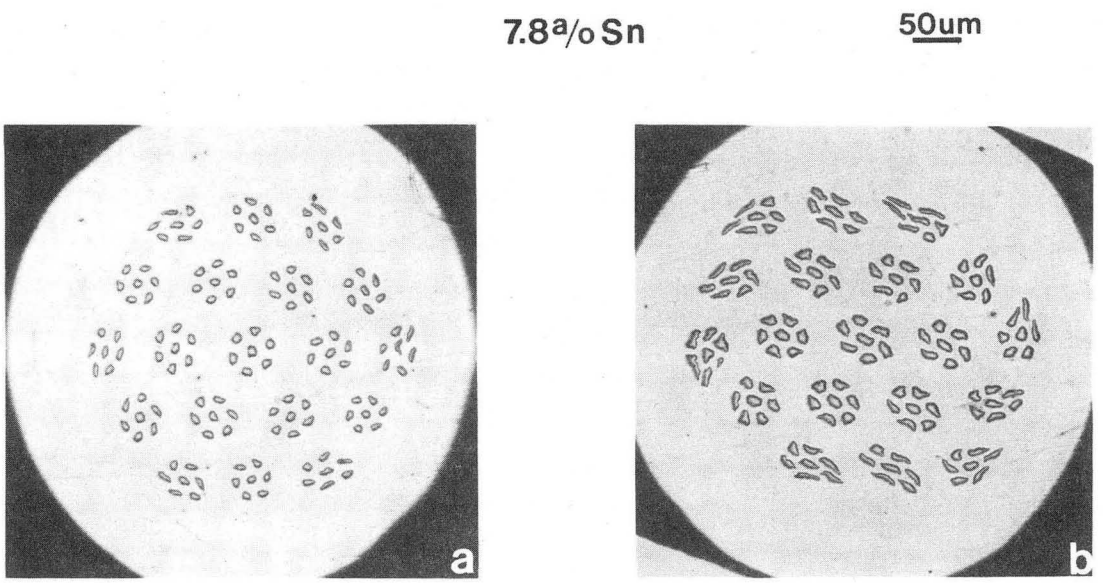

XBB 836-5038

Fig. 9b

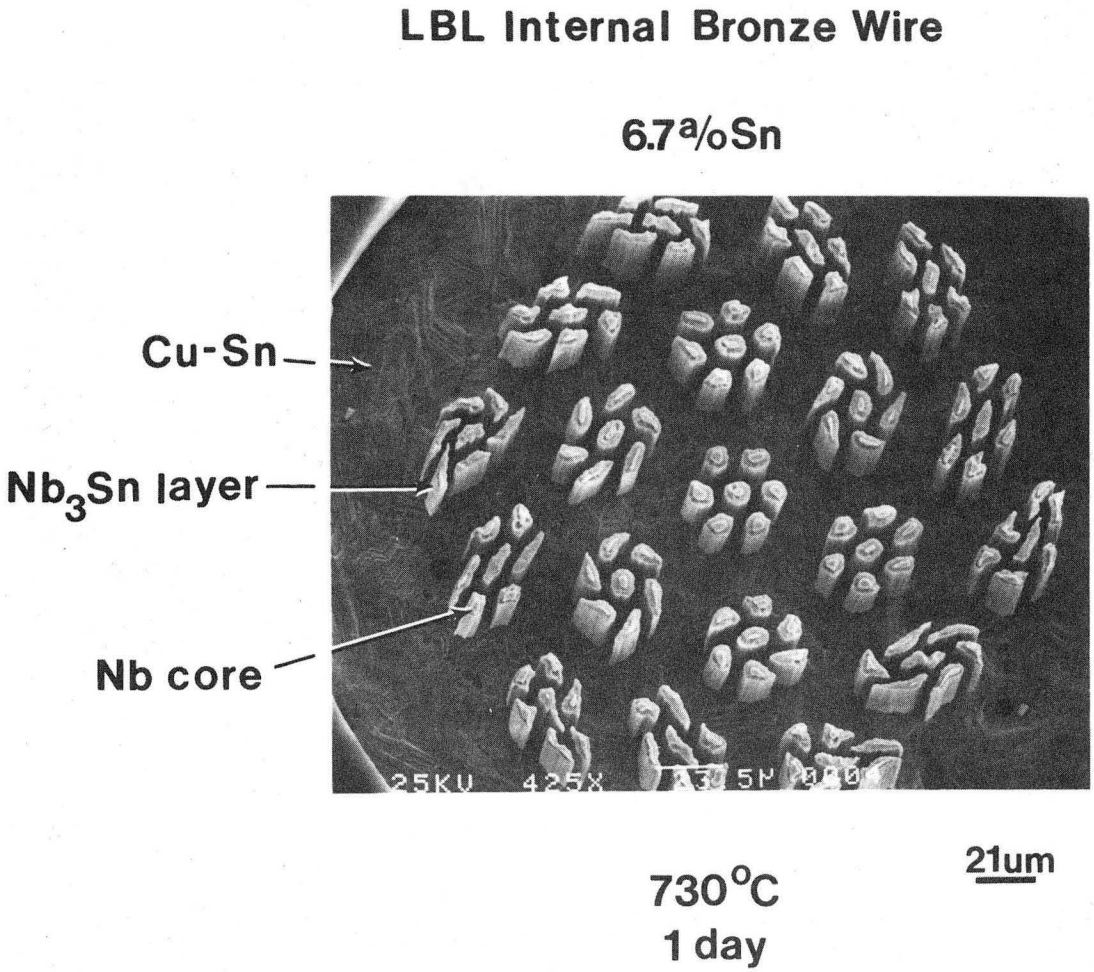
LBL Internal Bronze Wire
6.7a/oSn
Cu-Sn
Nb3Sn layer
Nb core
25KU 425X
21um
730°C
1 day
XBB 836-5039

Fig. 10

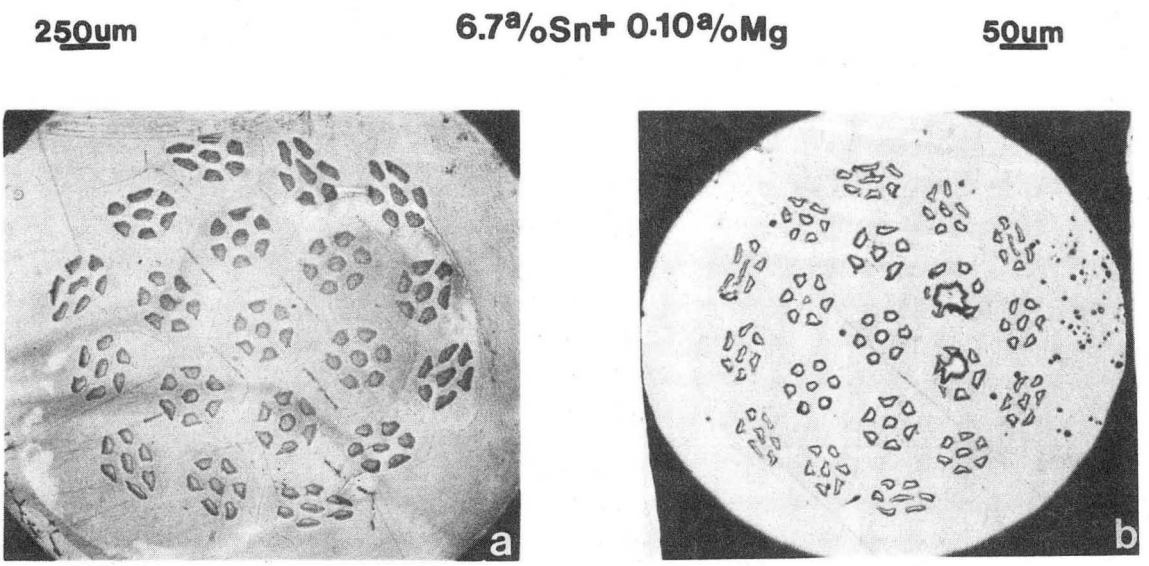

XBB 836-5037

Fig. 11

6.7 a/o Sn + 0.10 a/o Mg

Filament Modulation

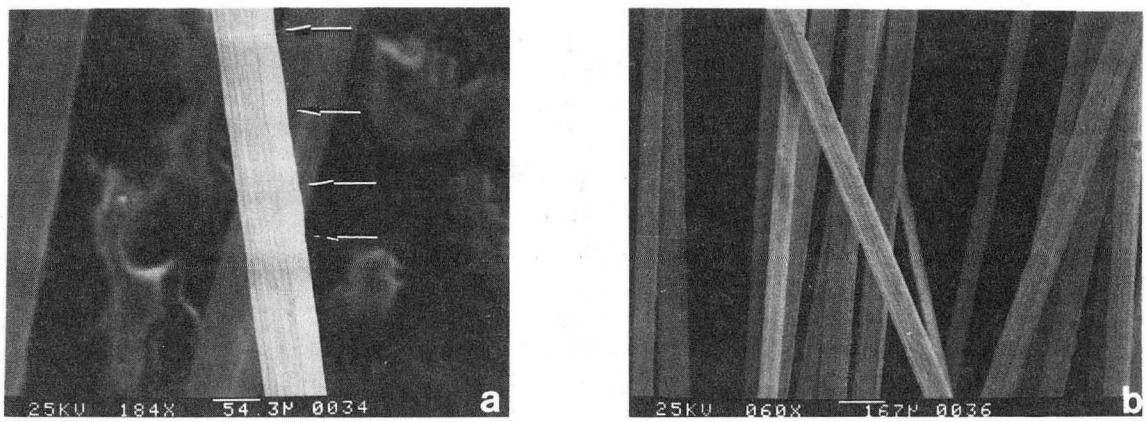

0.104 in
[2.65 mm]
Wire Diameter

XBB 836-5036

Fig. 12

6.7 a% Sn + 0.10 a% Mg

Modulations and Inclusions

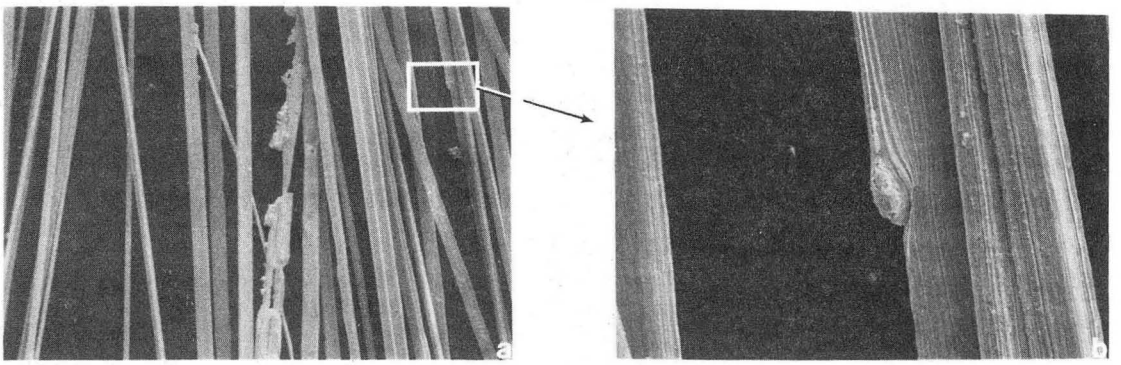

200um

0.040in
(1.0mm)
Wire Diameter

25um

XBB 836-5034

Fig. 13

Terminated Filament

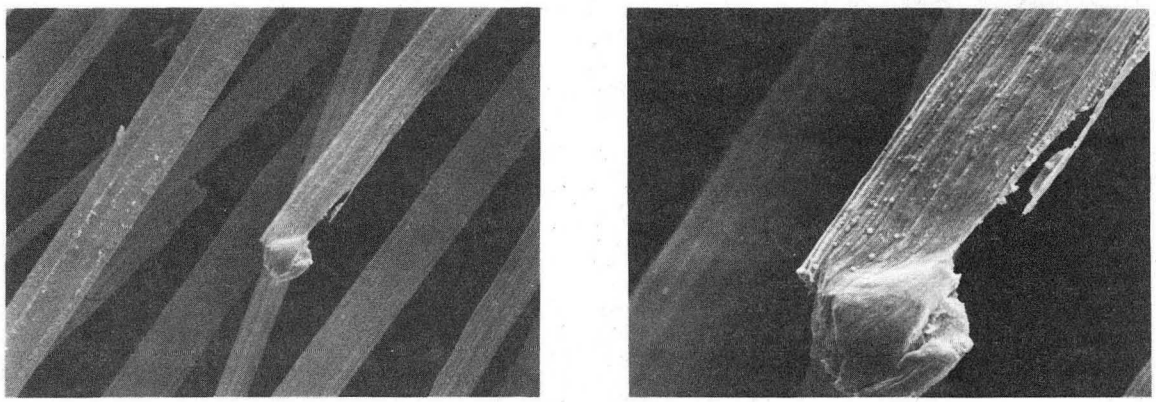

XBB 836-5033

Fig. 14

6.7 a/o Sn + 0.10 a/o Mg

Inclusions

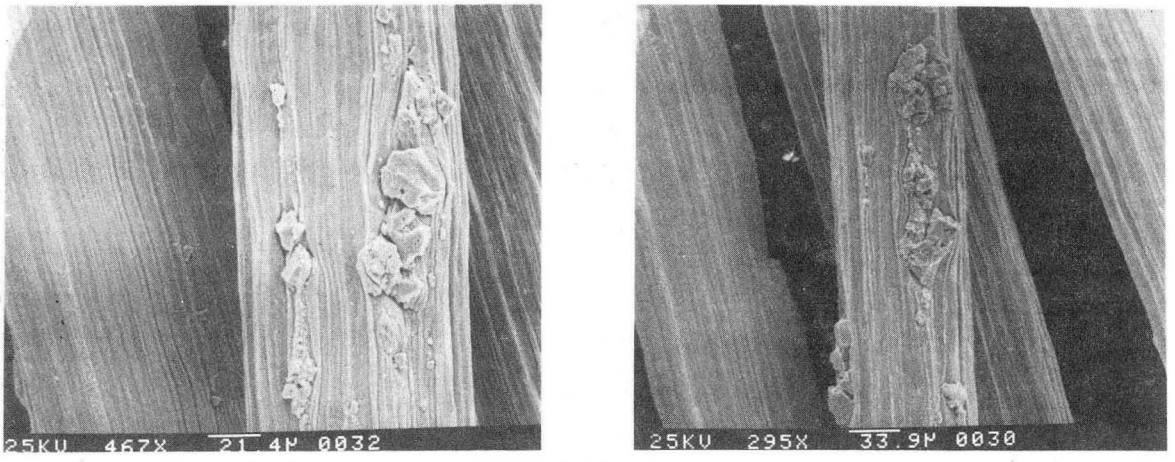

0.104 in
(2.65mm)
Wire Diameter

XBB 836-5032

Fig. 15

EDX of Inclusions
Only
Nb

6.7 a/o Sn + 0.10 a/o Mg

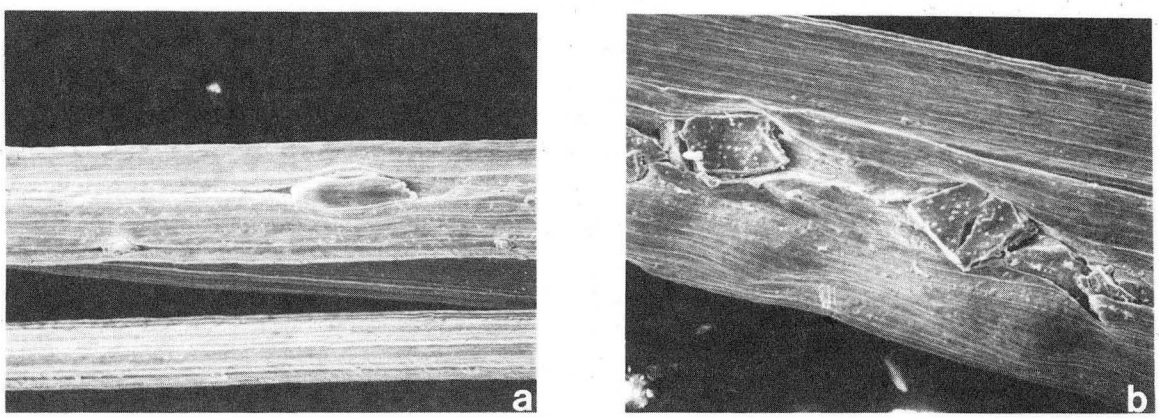

15um

0.040in
[1.0mm]
Wire Diameter

6um

XBB 836-5031

Fig. 16

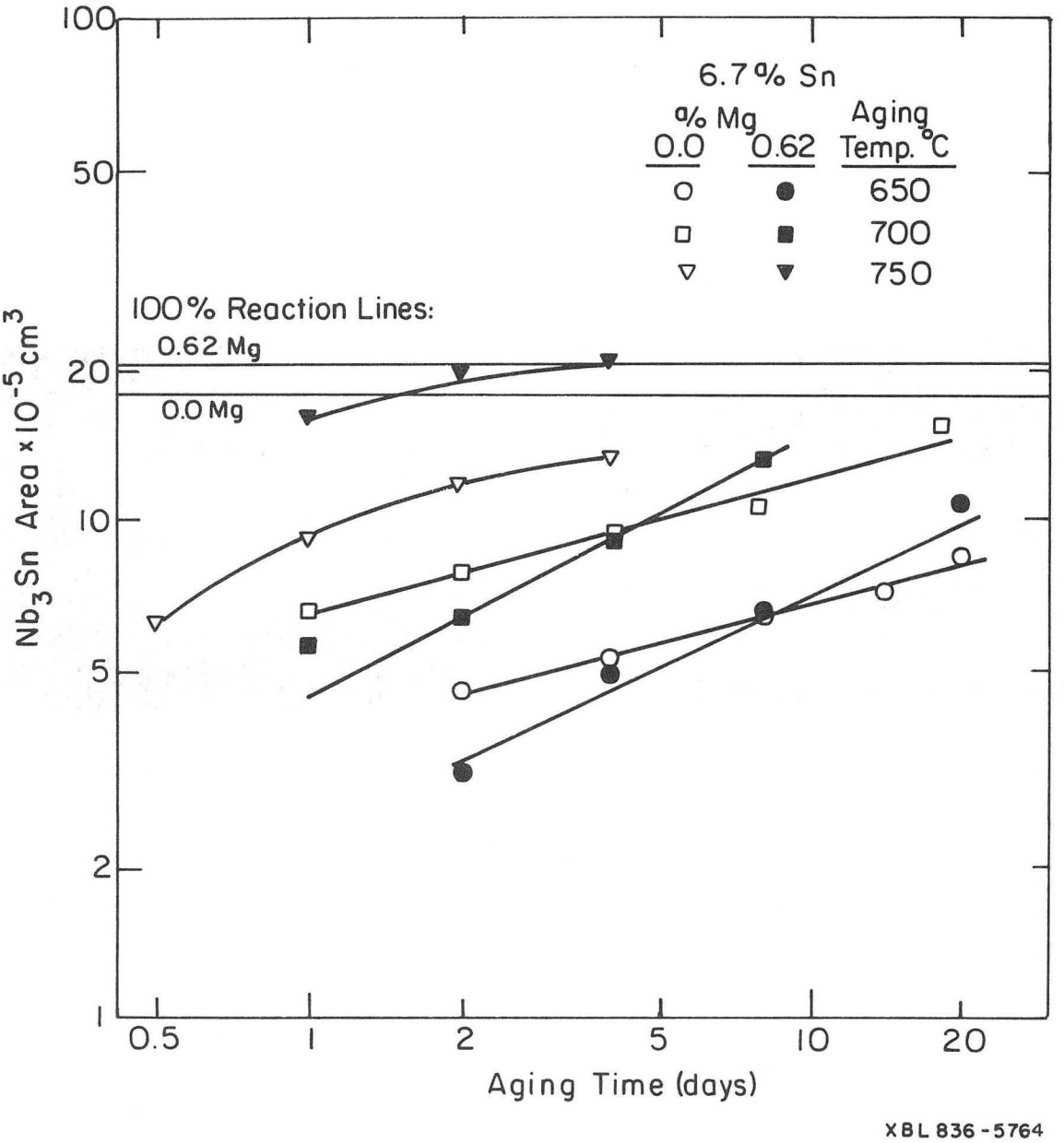
100
50
20
10
5
2
1
0.5
1
2
5
10
20
6.7% Sn
% Mg
0.0
0.62
Aging Temp. °C
650
700
750
100% Reaction Lines:
0.62 Mg
0.0 Mg
Nb3Sn Area x10-5 cm3
Aging Time (days)
XBL 836-5764

Fig. 17

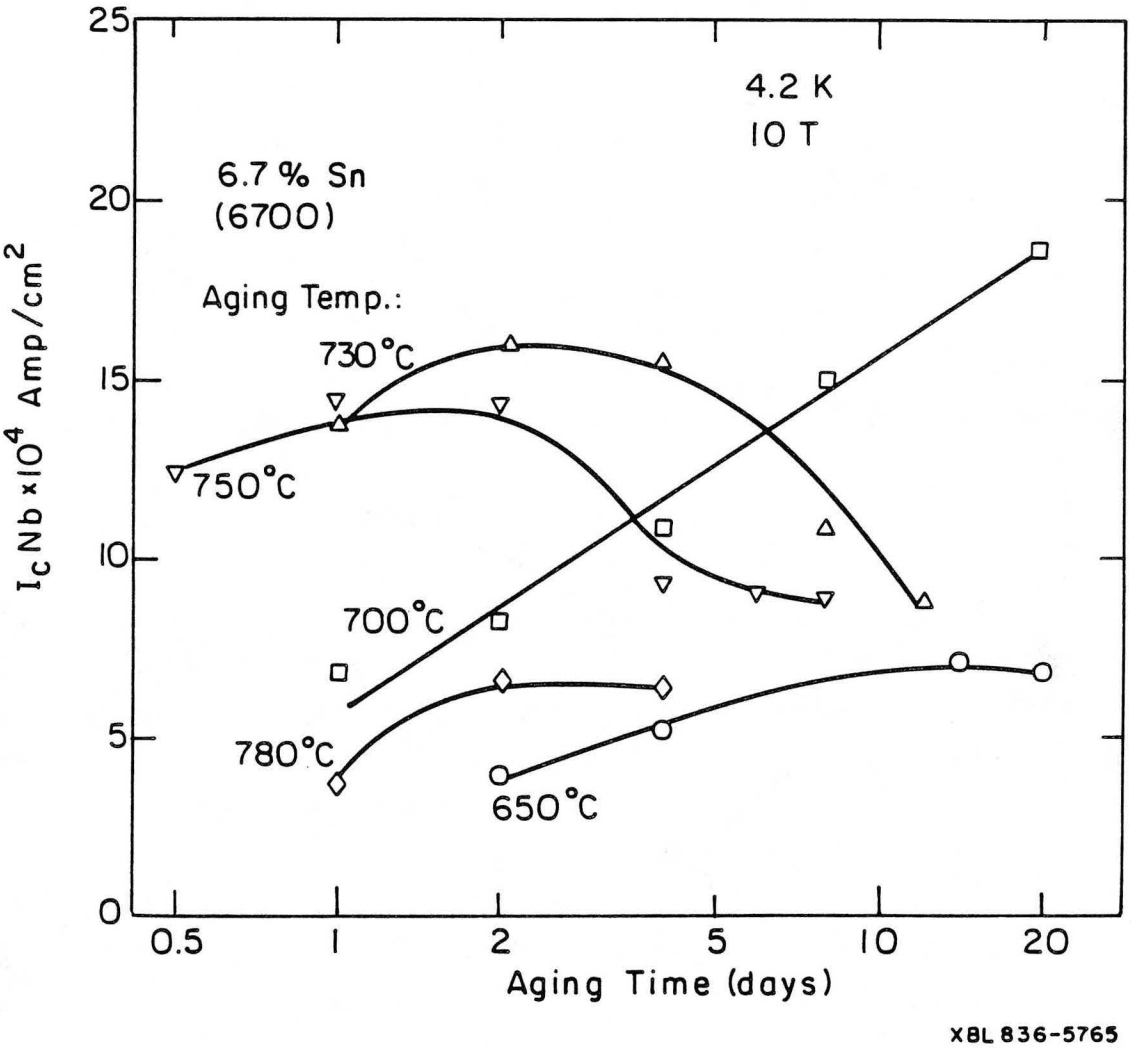
4.2 K
10 T
6.7 % Sn
(6700)
Aging Temp.:
730°C
750°C
700°C
780°C
650°C
I_c Nb x 10^4 Amp/cm^2
Aging Time (days)
0
5
10
15
20
25
0.5
1
2
5
10
20
X8L 836-5765

Fig. 18

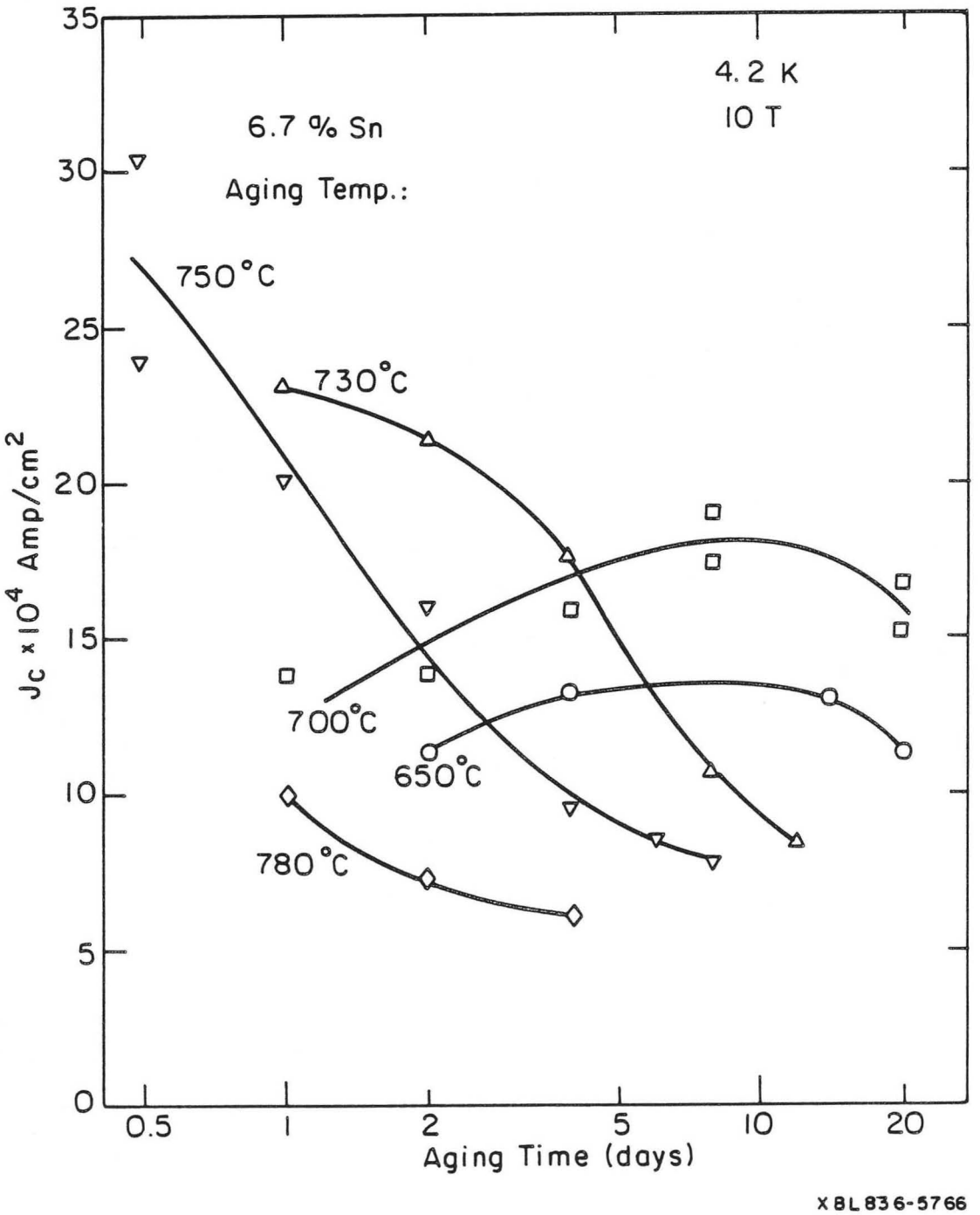
4.2 K
10 T
6.7 % Sn
Aging Temp.:
750°C
730°C
700°C
650°C
780°C
$J_c \times 10^4$ Amp/cm^2
Aging Time (days)
0
5
10
15
20
25
30
35
0.5
1
2
5
10
20
XBL836-5766

Fig. 19

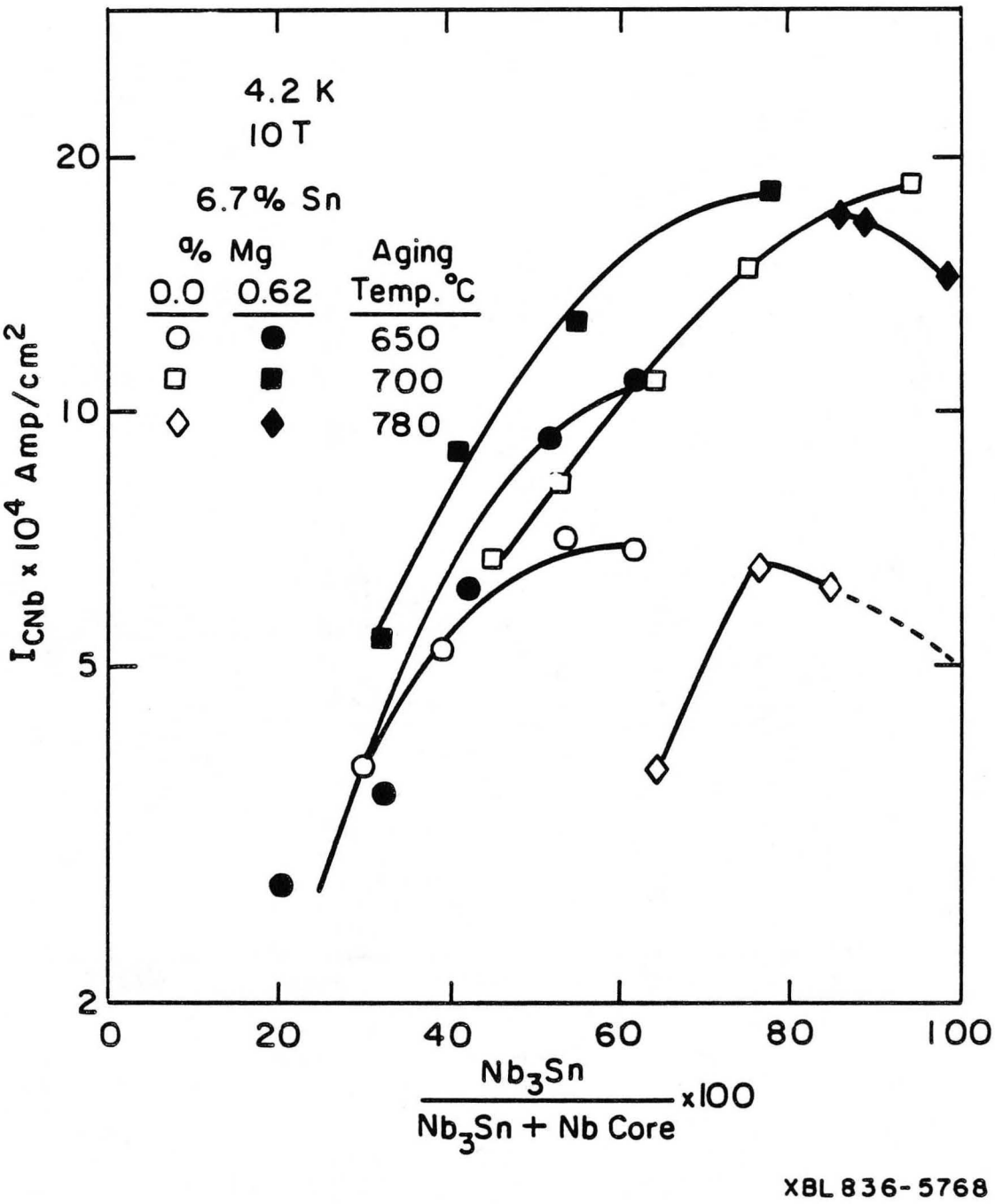
4.2 K
10 T
6.7% Sn
% Mg
0.0
0.62
Aging Temp. °C
650
700
780
$I_{CNb} \times 10^4$ Amp/cm^2
20
10
5
2
0
20
40
60
80
100
$\frac{Nb_3Sn}{Nb_3Sn + Nb\ Core} \times 100$
XBL 836-5768

Fig. 20a

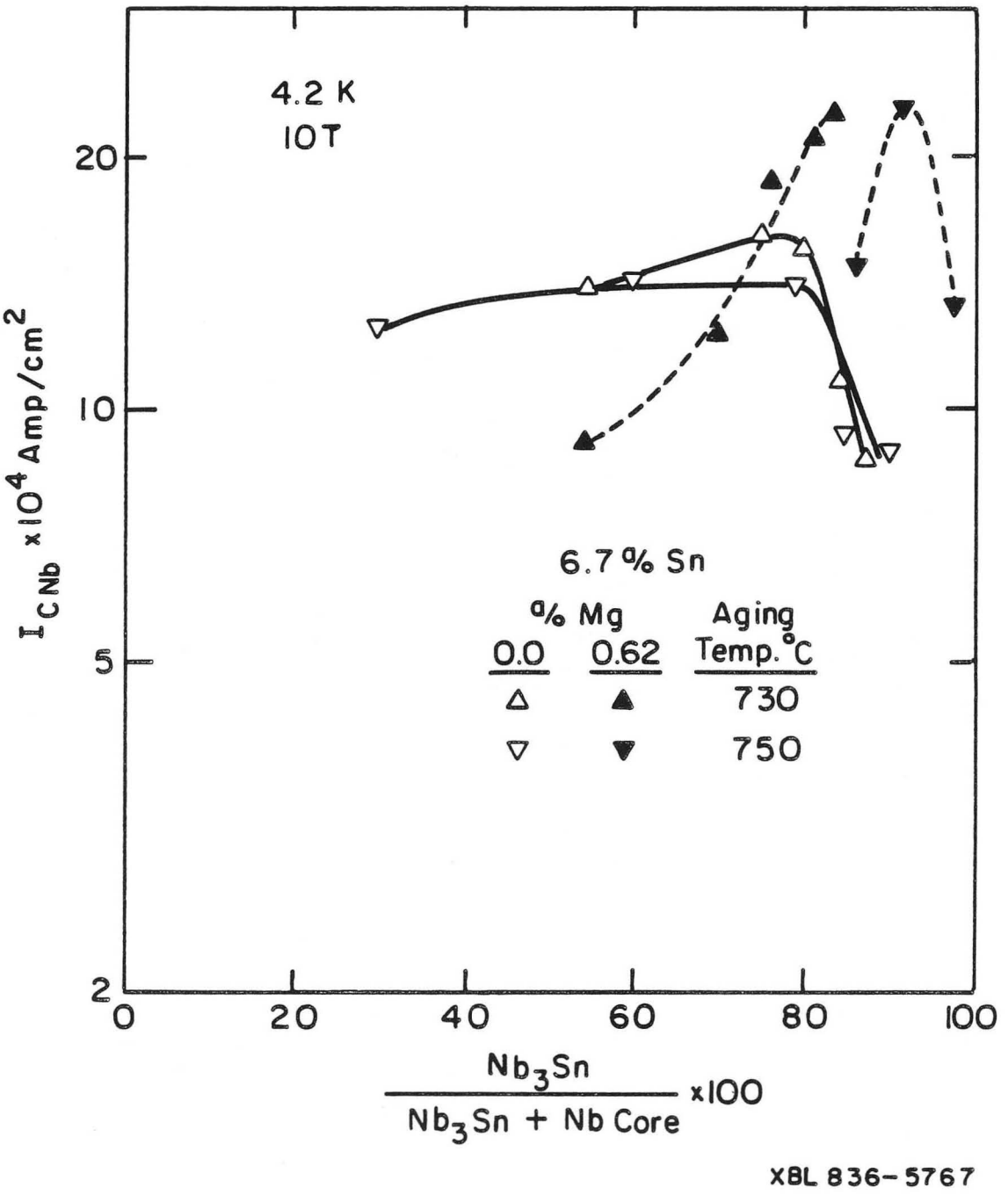
4.2 K
10T
20
10
5
2
I_{CNb} x 10^4 Amp/cm^2
6.7% Sn
% Mg
0.0
0.62
Aging Temp. °C
730
750
0
20
40
60
80
100
$\frac{Nb_3Sn}{Nb_3Sn + Nb\ Core}$ x100
XBL 836-5767

Fig. 20b

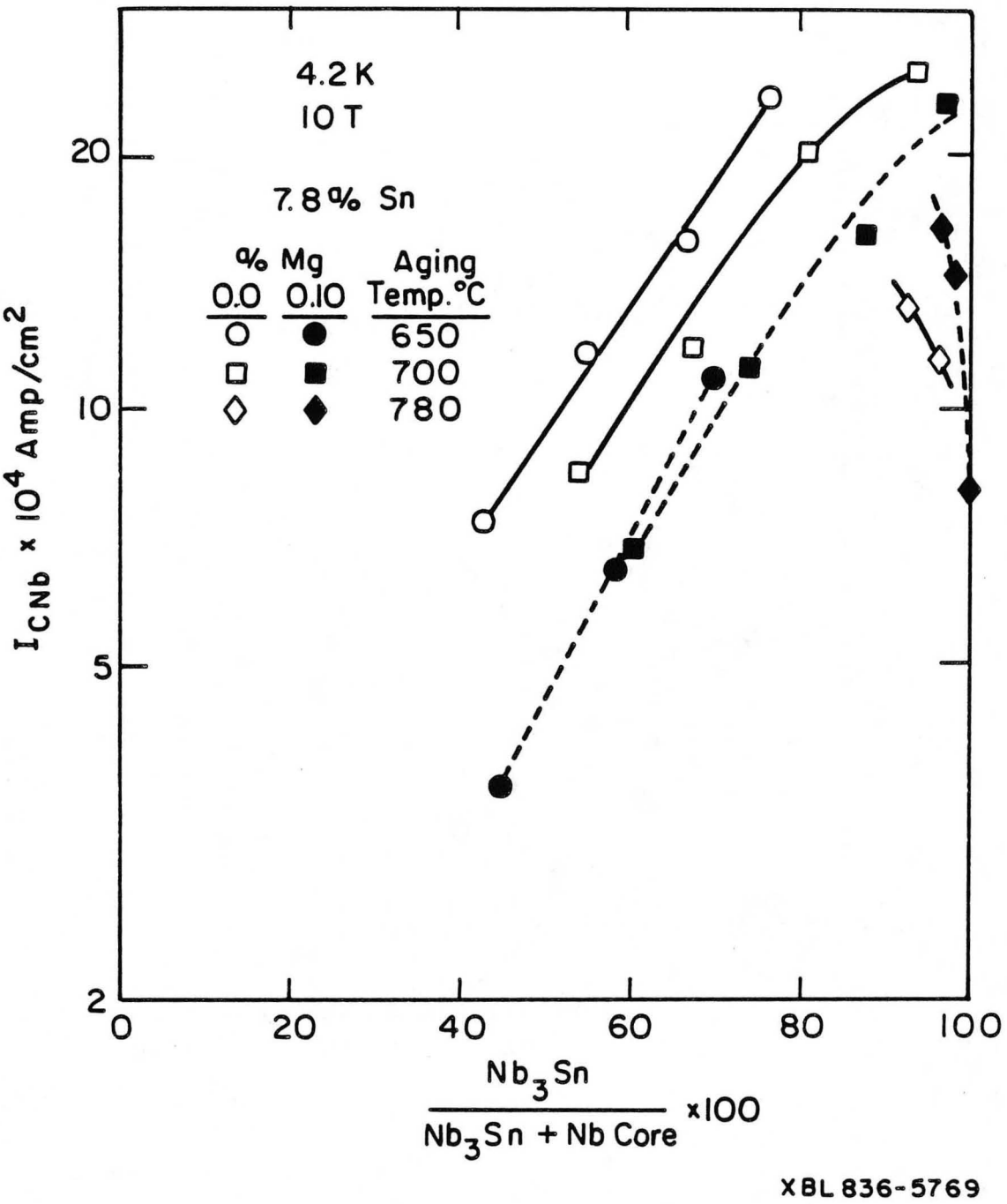
4.2 K
10 T
7.8% Sn
% Mg
0.0
0.10
Aging Temp. °C
650
700
780
$I_{CNb} \times 10^4$ Amp/cm^2
20
10
5
2
0
20
40
60
80
100
$\frac{Nb_3Sn}{Nb_3Sn + Nb\ Core} \times 100$
XBL 836-5769

Fig. 20c

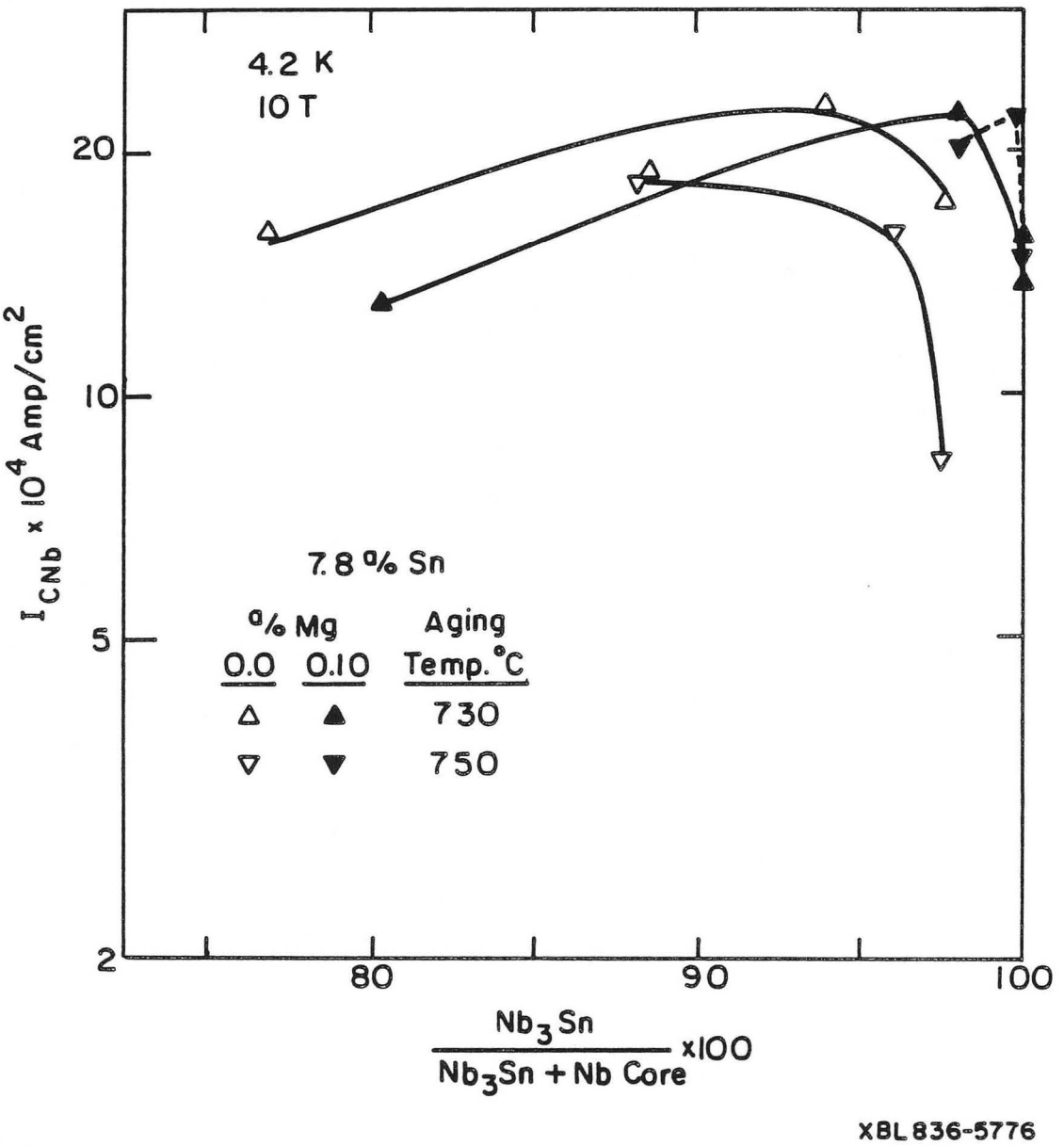
4.2 K
10 T
20
10
5
2
$I_{CNb} \times 10^4$ Amp/cm^2
7.8 % Sn
% Mg
0.0
0.10
Aging Temp. °C
730
750
80
90
100
$\frac{Nb_3Sn}{Nb_3Sn + Nb\ Core} \times 100$
XBL 836-5776

Fig. 20d

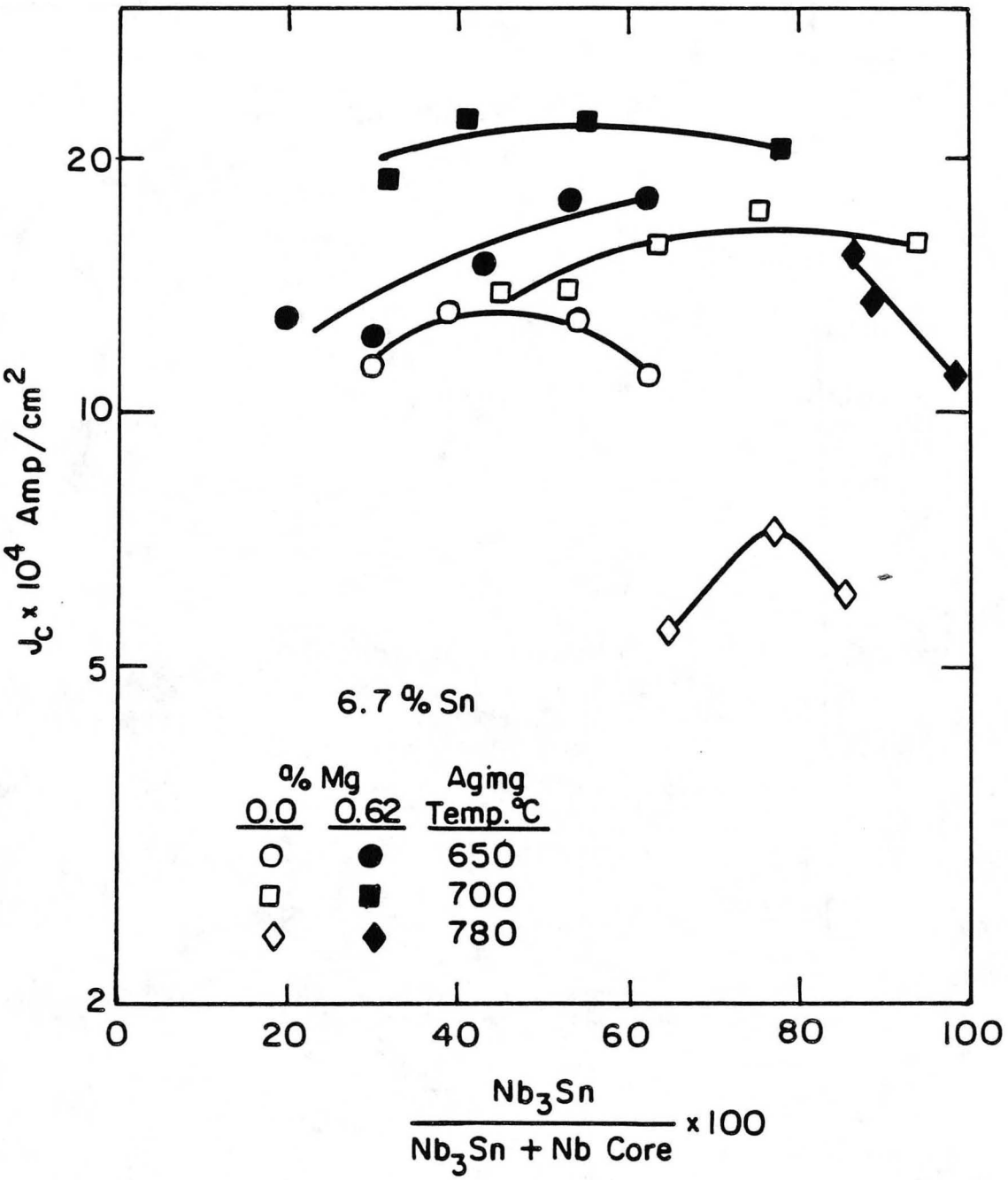
20
10
5
2
$J_c \times 10^4$ Amp/cm^2
6.7 % Sn
% Mg
0.0
0.62
Aging Temp. °C
650
700
780
0
20
40
60
80
100
$\frac{Nb_3Sn}{Nb_3Sn + Nb\ Core} \times 100$
XBL836-5770

Fig. 21a

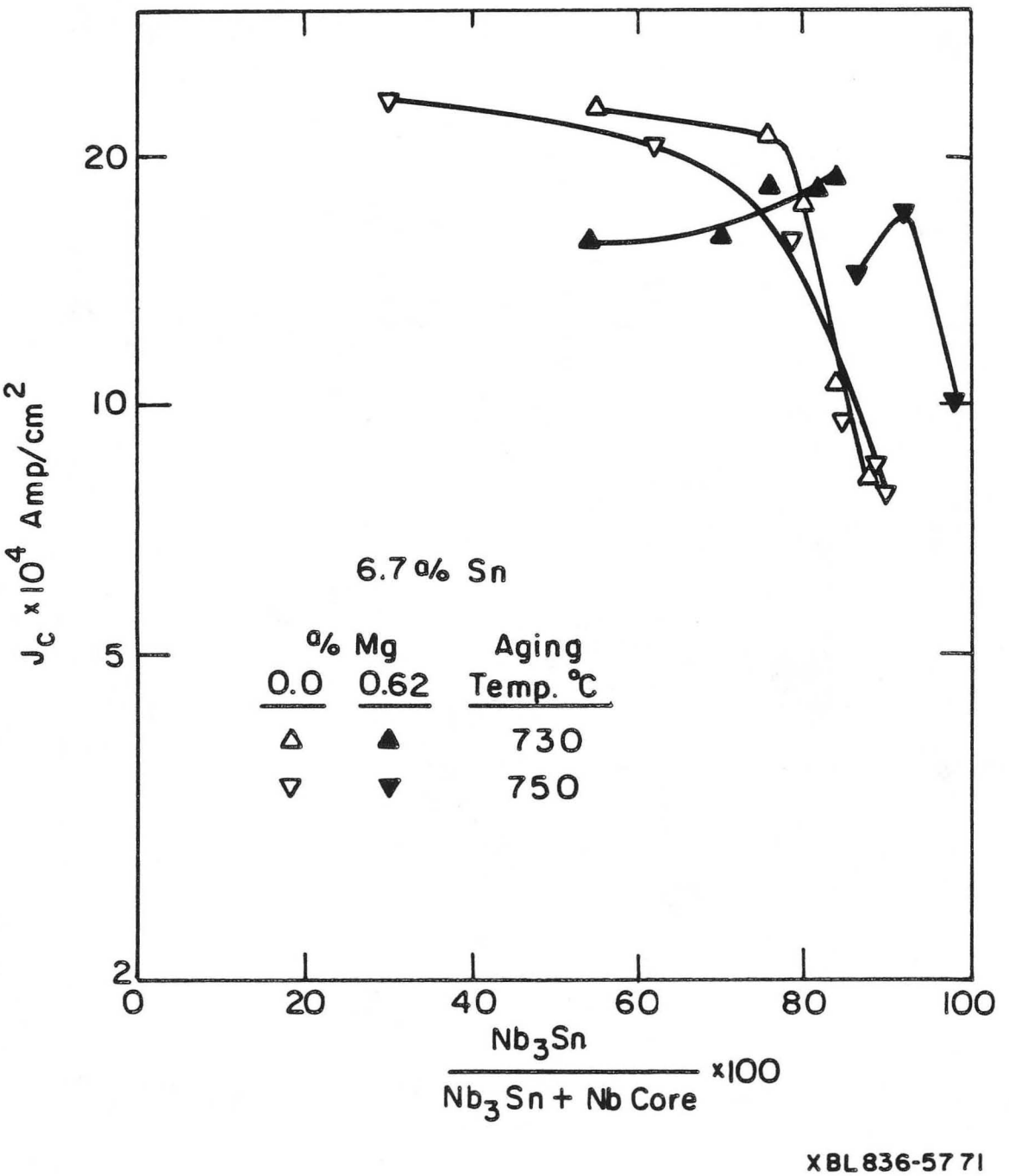
20
10
5
2
$J_c \times 10^4$ Amp/cm^2
6.7 a/o Sn
a/o Mg
0.0
0.62
Aging Temp. °C
730
750
0
20
40
60
80
100
$\frac{Nb_3Sn}{Nb_3Sn + Nb\ Core} \times 100$
XBL836-5771

Fig. 21b

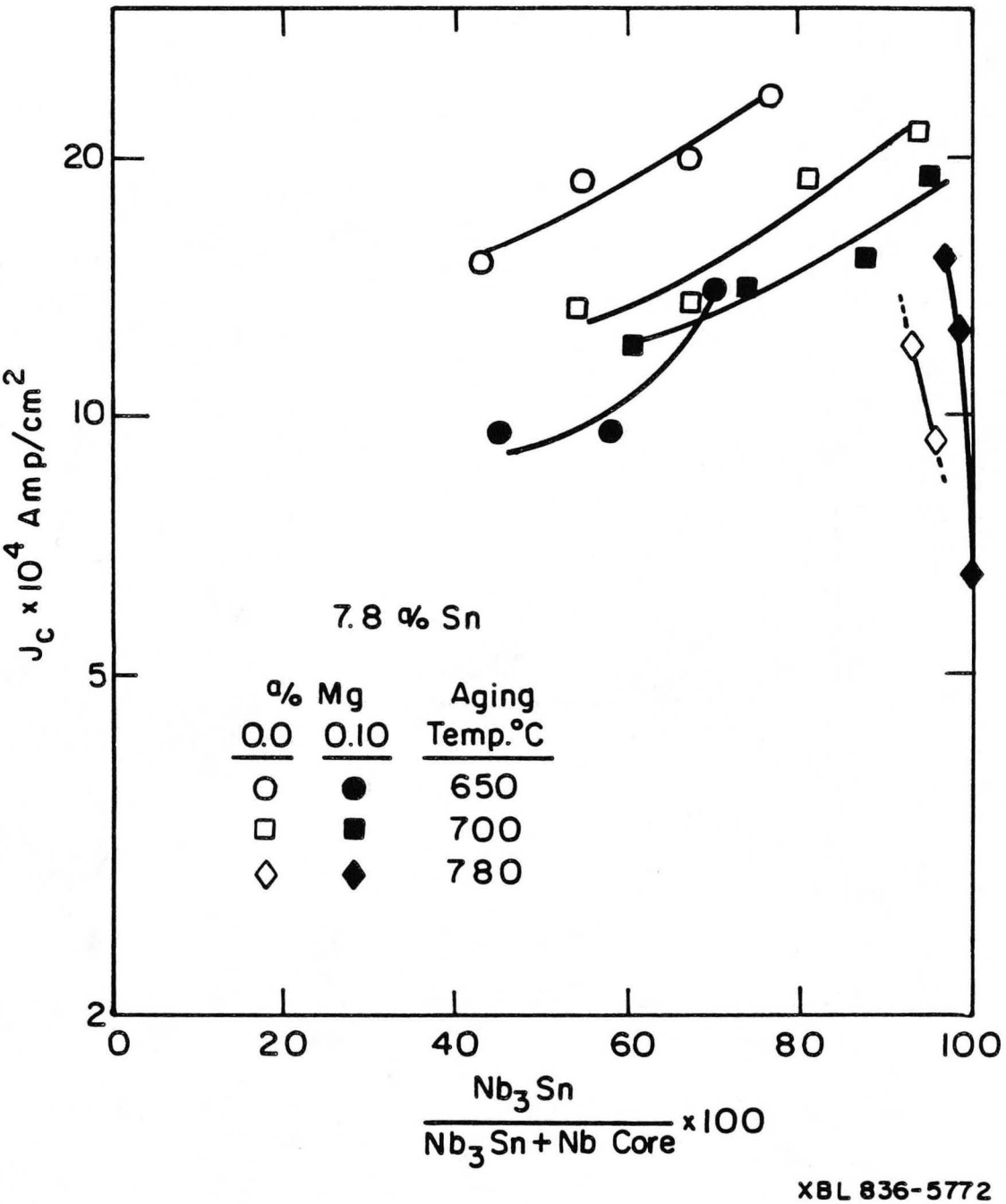
20
10
5
2
$J_c \times 10^4$ Amp/cm^2
7.8 % Sn
% Mg
0.0
0.10
Aging Temp.°C
650
700
780
0
20
40
60
80
100
$\frac{Nb_3Sn}{Nb_3Sn + Nb\ Core} \times 100$
XBL 836-5772

Fig. 21c

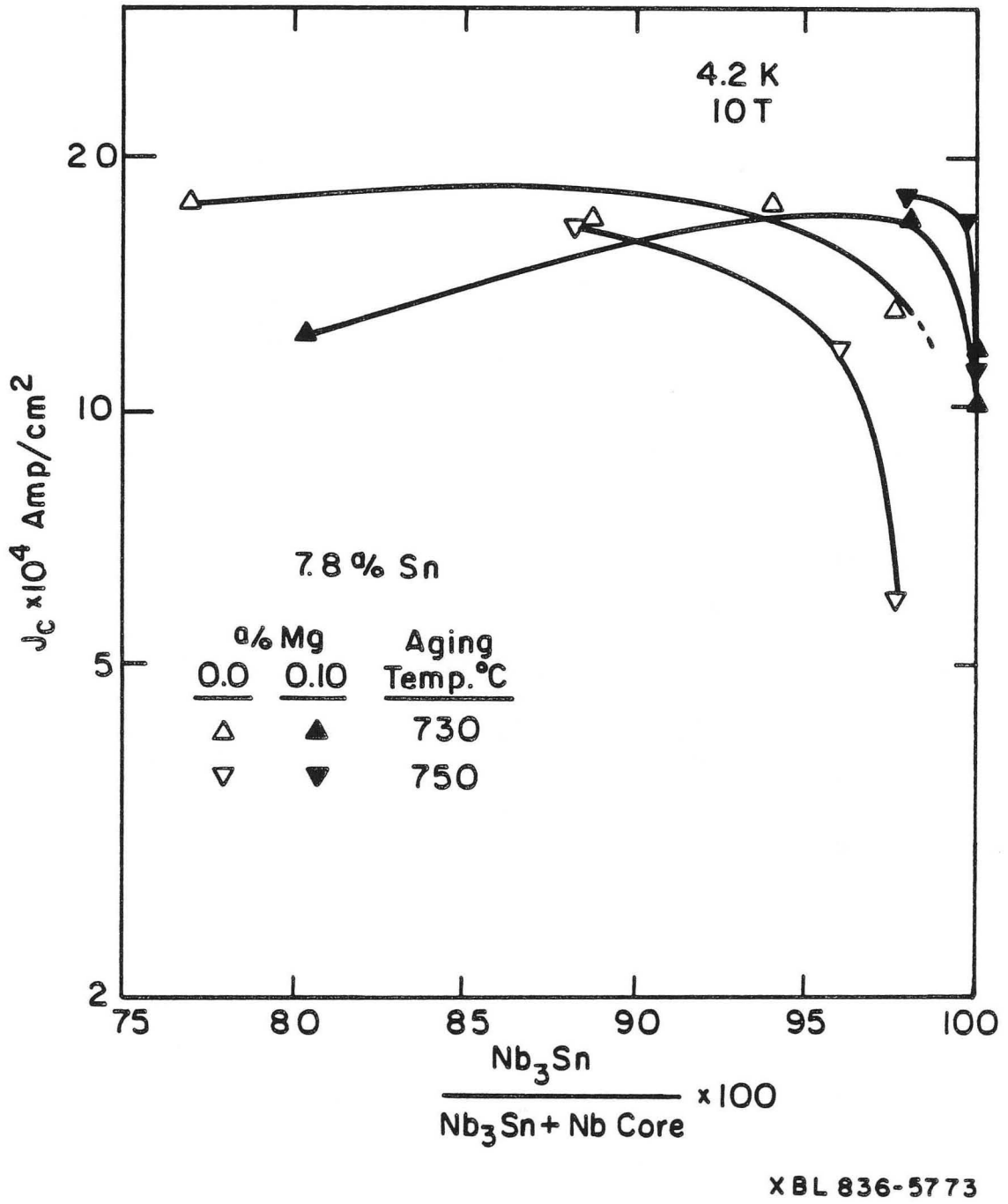
4.2 K
10 T
20
10
5
2
$J_c \times 10^4$ Amp/cm^2
7.8% Sn
% Mg
0.0
0.10
Aging Temp.°C
730
750
75
80
85
90
95
100
$\frac{Nb_3Sn}{Nb_3Sn + Nb\ Core} \times 100$
XBL 836-5773

Fig. 21d

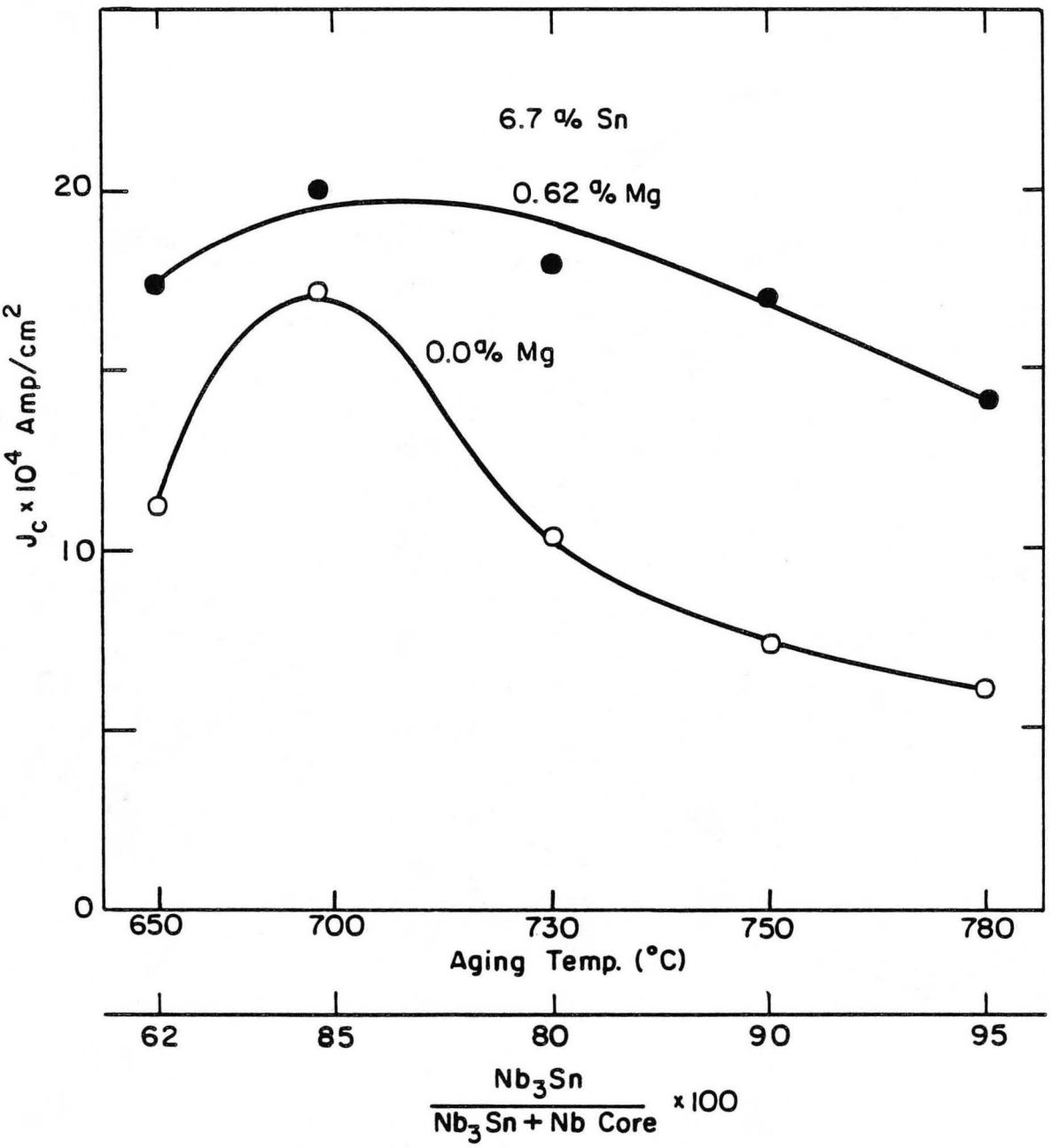
6.7 % Sn
0.62 % Mg
0.0% Mg
20
10
0
$J_c \times 10^4$ Amp/cm^2
650
700
730
750
780
Aging Temp. (°C)
62
85
80
90
95
$\frac{Nb_3Sn}{Nb_3Sn + Nb\ Core} \times 100$
XBL 836-5774

Fig. 22

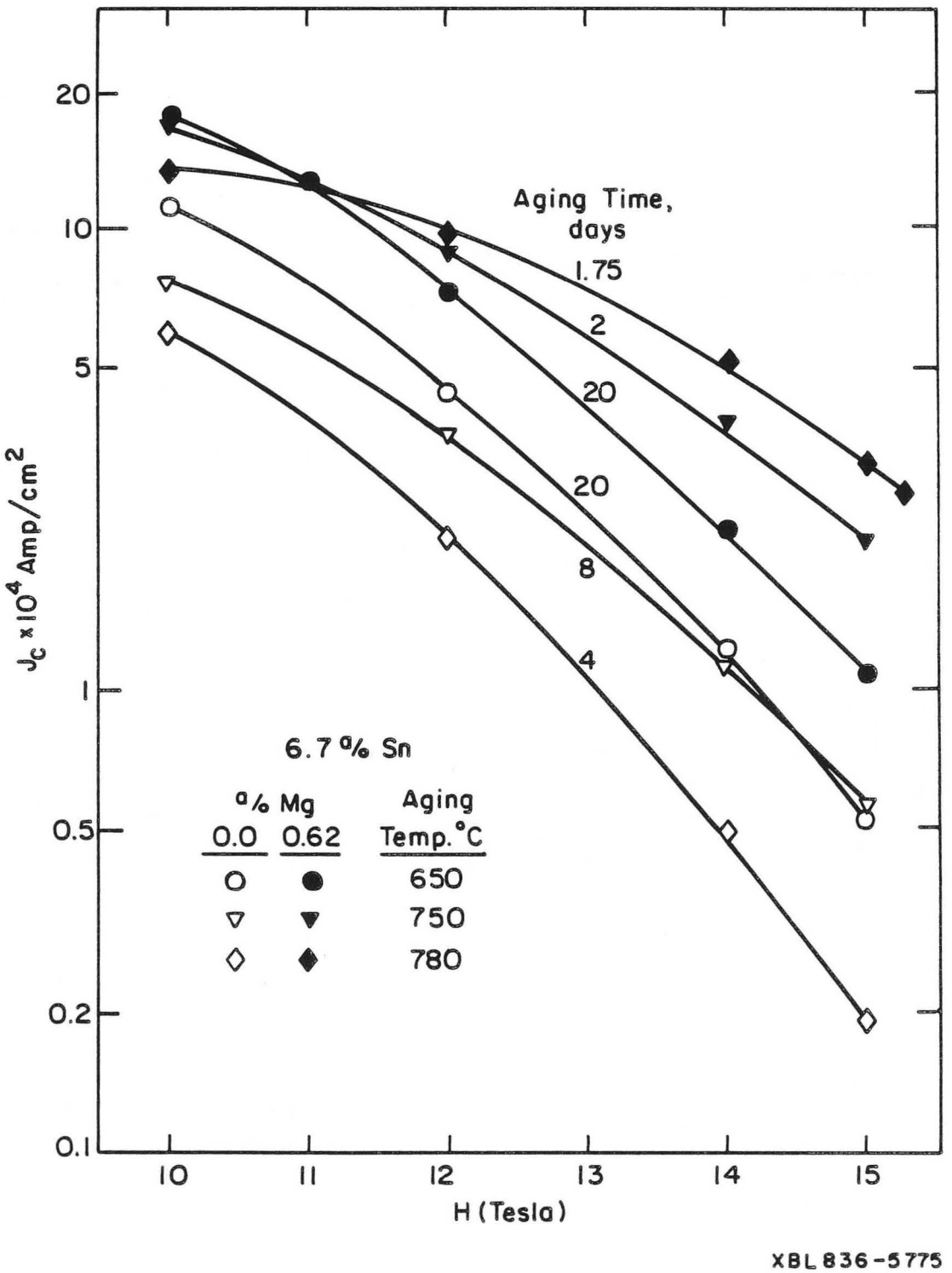
20
10
5
1
0.5
0.2
0.1
$J_c \times 10^4$ Amp/cm^2
10
11
12
13
14
15
H (Tesla)
Aging Time, days
1.75
2
20
20
8
4
6.7 % Sn
% Mg
0.0
0.62
Aging Temp. °C
650
750
780
XBL 836-5775

Fig. 23

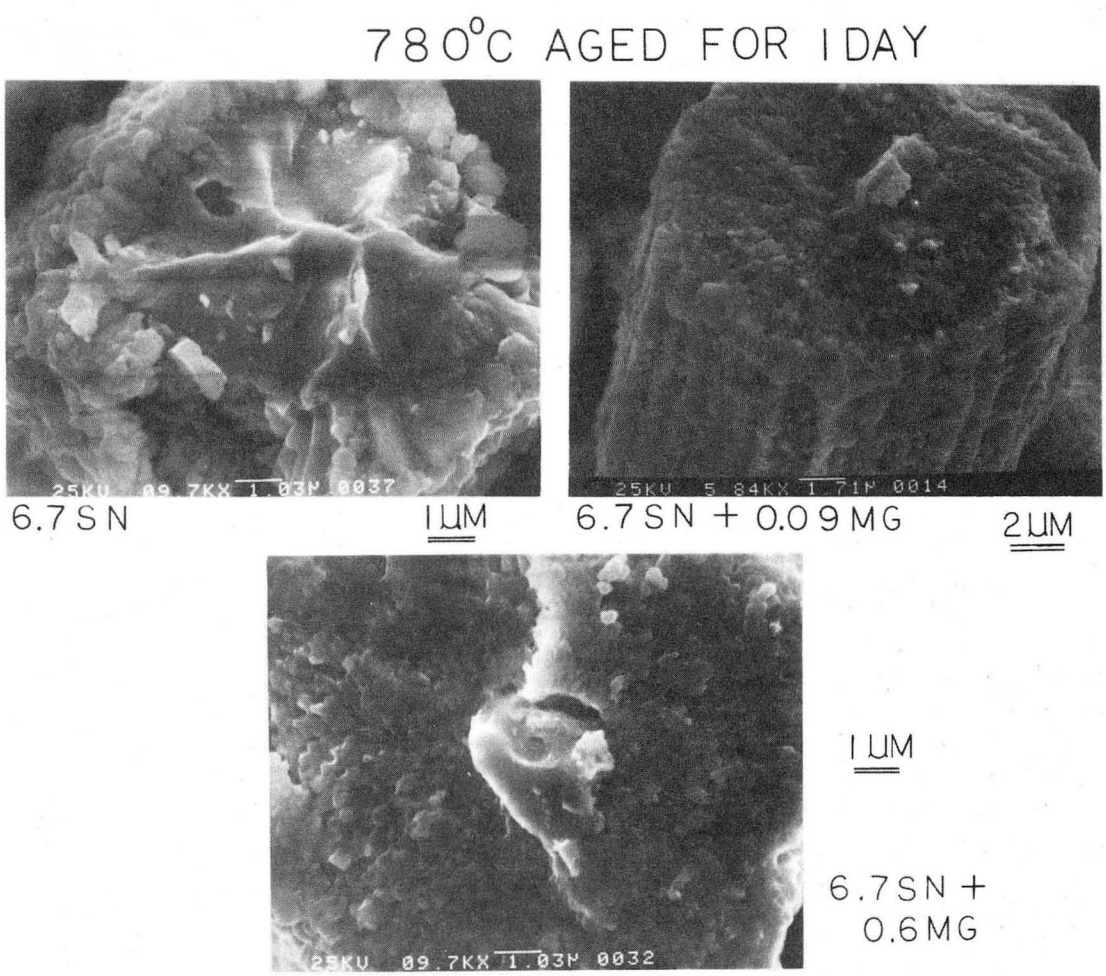

XBB 820-10447

Fig. 24

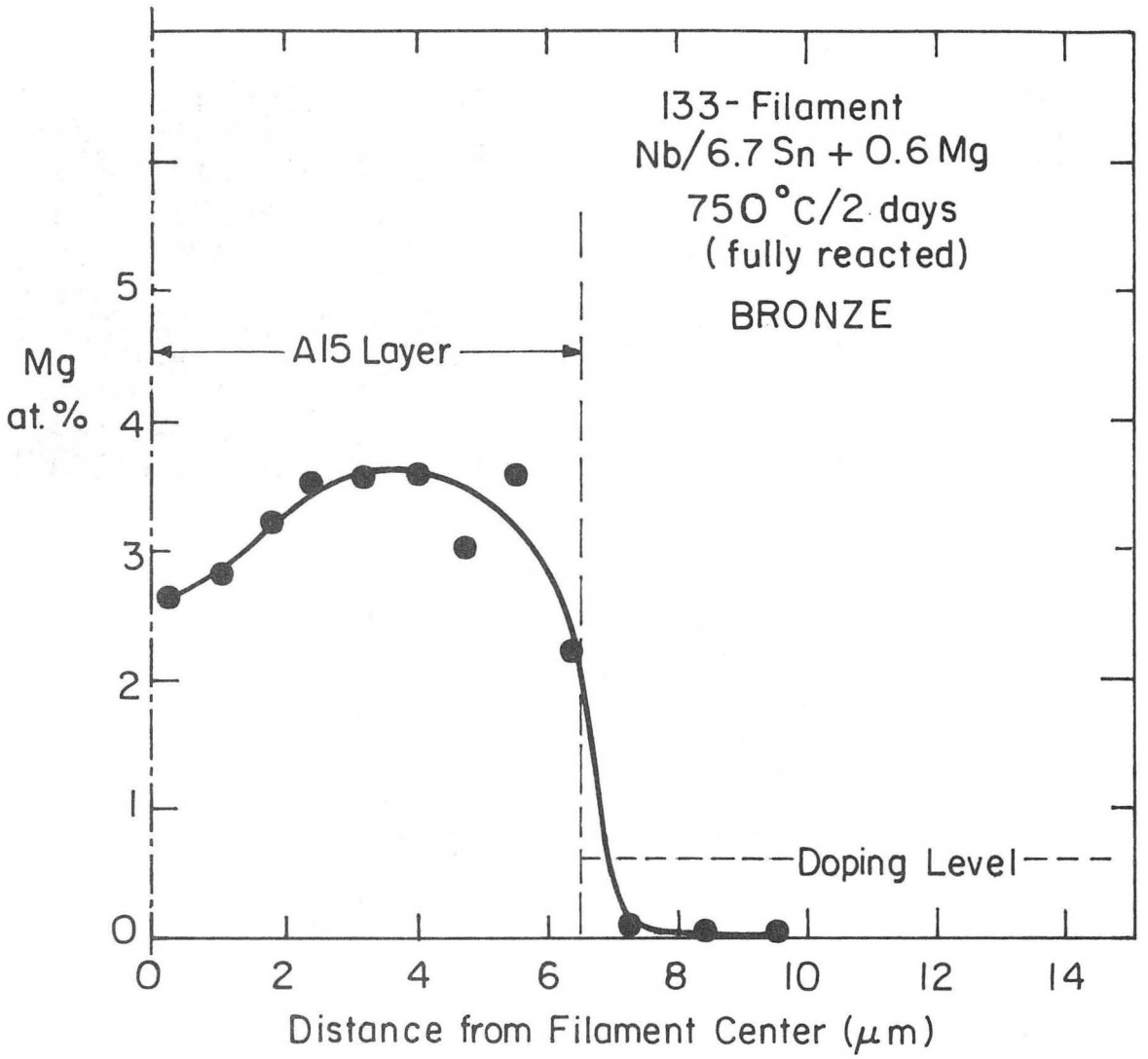
133- Filament
Nb/6.7 Sn + 0.6 Mg
750°C/2 days
(fully reacted)
BRONZE
A15 Layer
Doping Level
Mg
at. %
0
1
2
3
4
5
0
2
4
6
8
10
12
14
Distance from Filament Center (μm)
XBL 8211-6825

Fig. 25

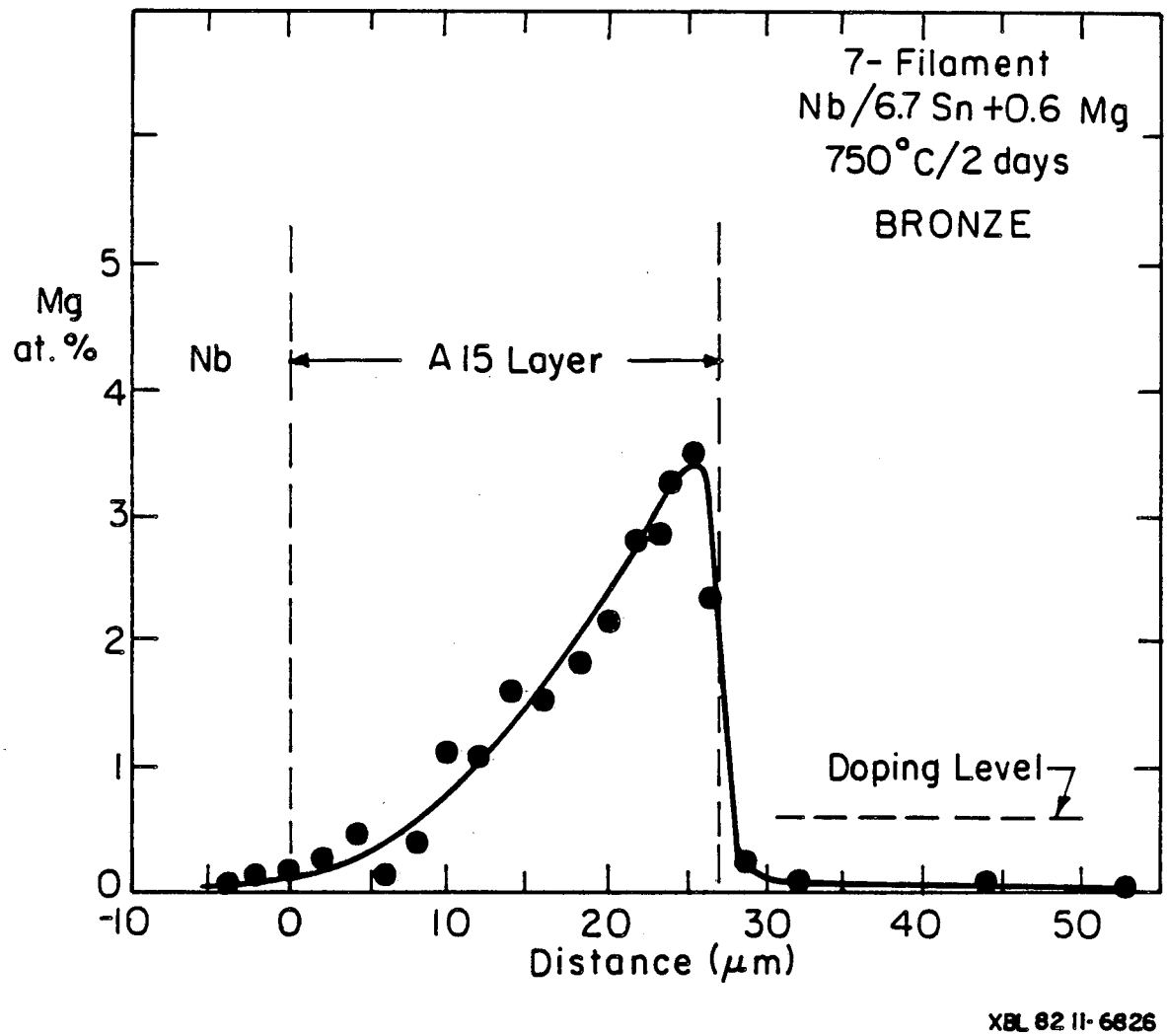
7- Filament
Nb/6.7 Sn +0.6 Mg
750°C/2 days
BRONZE
Mg
at. %
Nb
A 15 Layer
Doping Level
Distance (μm)
XBL 82 11-6826

Fig. 26

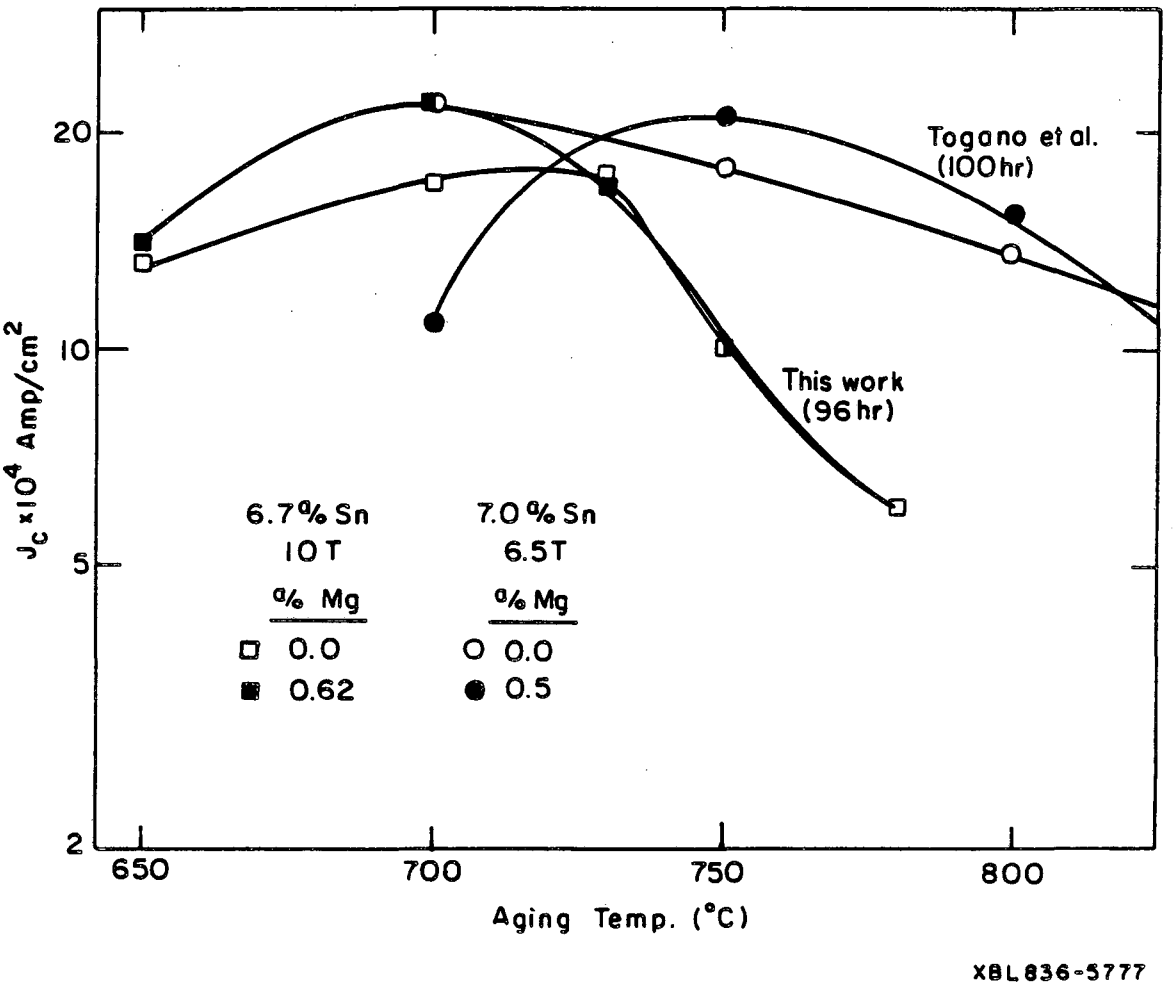
20
10
5
2
650
700
750
800
Aging Temp. (°C)
$J_c \times 10^4$ Amp/cm^2
Togano et al.
(100hr)
This work
(96hr)
6.7% Sn
10 T
% Mg
0.0
0.62
7.0 % Sn
6.5T
% Mg
0.0
0.5
XBL836-5777

Fig. 27

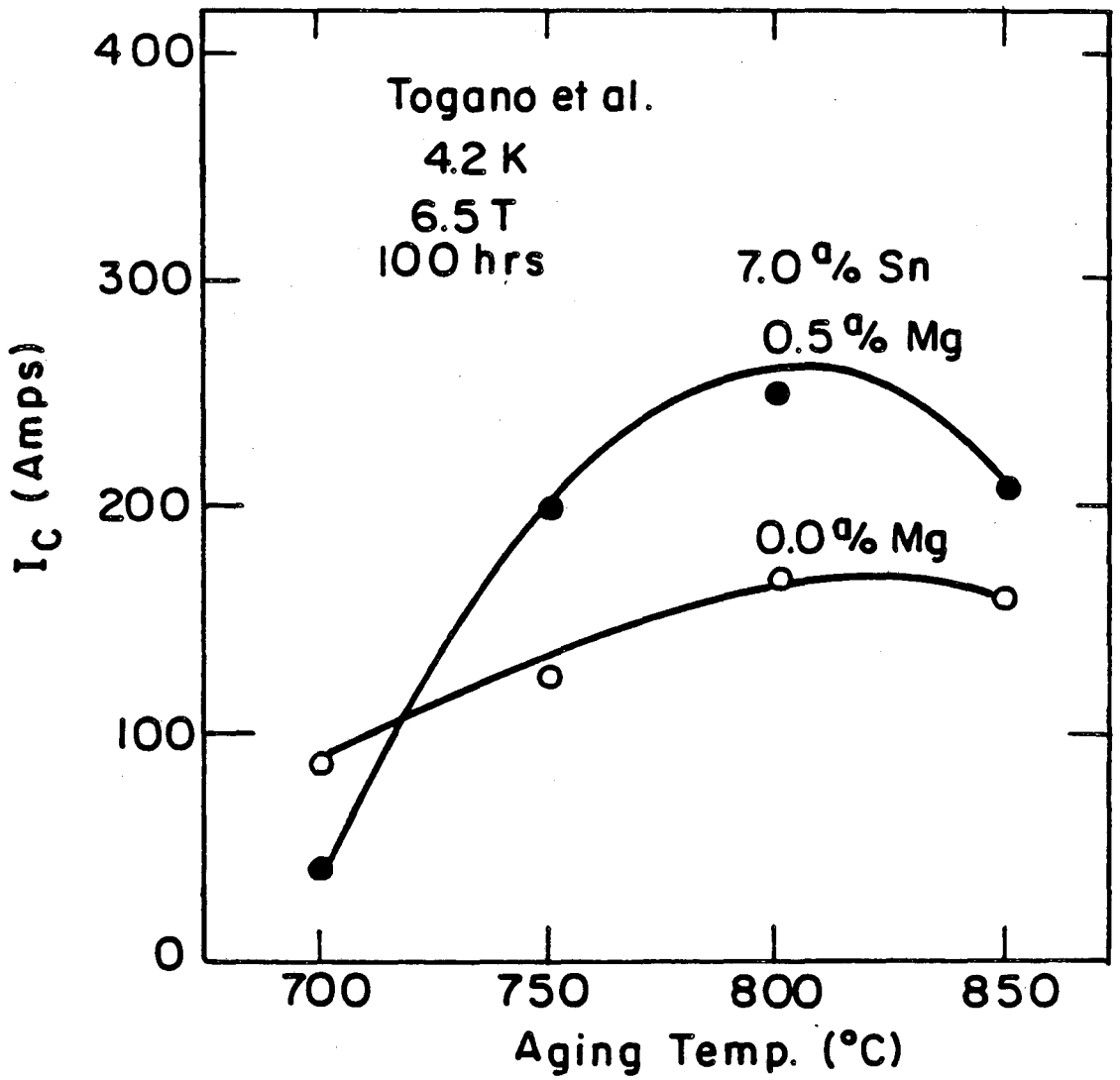
Togano et al.
4.2 K
6.5 T
100 hrs
7.0 % Sn
0.5 % Mg
0.0 % Mg
I_c (Amps)
400
300
200
100
0
700
750
800
850
Aging Temp. (°C)
XBL 836-5779

Fig. 28

Appendix

Bronze Ingot Manufacture

It was determined that the ingots with the least tin gradient along their length also had a uniform hardness along their length. Cooling the ingot from above the liquidus produced this uniformity. Evidently the segregation was kept to a minimum by cooling the quartz ampoule in water. Coring could be removed by a solution treatment but a large varation along the ingot could not.

The addition of Mg to the melt increases the as cast and post homogenization hardness of the ingot. The effect of Mg on the cast structure is not known. Of importance are the inter-dentritic spacing and the grain size and grain structure. The effect of Mg on the microstructural state of the bronze was not throroughly studied. The method of ingot manufacture is subject to the experimenter's judgment as to furnace holding time and ingot cooling rate. The important parameters are yet to be determined.

If the cast material was form-rolled without homogenization, it cracked. The ingots failed in two ways. First, cracks formed normal to the rolling direction at the ingot-roller contact surface. The second was by alligatoring. Some homogenized ingots of higher Mg composition also failed in the above manner. The post homogenization grain size of the high Mg-bronze is larger than the Mg-free bronze; as a result, ductility was reduced. By lowering the solution temperature from 750°C to 700°C cracking was eliminated.

Bronze Ductility

A study of the bronze tube material was initiated to determine the origin of the ductility differences between the wires. Bronze rod material which remanined after tube manufacure was used. The rods were work hardened by a 10% reduction in area (by swaging) for easy machining for tube fabrication. The rods were first annealed at 450°C for 1hr. The hardness at first drops with the addition of Mg, but then it increases to values much higher than Mg-free ingots (Table I). This type of hardness variation is common for systems doped with elements which have a high affinity for oxygen. To eliminate or reduce the effect of grain size on hardness the bars were given a solution treatment at 750°C for 12hrs. The hardness of every material dropped with all of the Mg-bronze values about the same. To determine if the hardness variation in the low temperature anneal was due to precipitate hardening another low temperature anneal was done. The hardnesses of the low Mg and Mg-free bronze material remained the same, while that of the high Mg bronze increased substantially, indicating that dispersion or precipitate hardening may be occurring in the high Mg-bronze.

LAWRENCE BERKELEY LABORATORY
TECHNICAL INFORMATION DEPARTMENT
UNIVERSITY OF CALIFORNIA
BERKELEY, CALIFORNIA 94720